Hydraulics Laboratory

Civil Engineering Department

Katholieke Universiteit Leuven

ANALYSIS OF NEAR-WALL TURBULENCE MODELLING WITH k-ε MODELS

Report No. HYD/ET/00/COSINUS2

December 2000

Erik A. TOORMAN

A contribution to the MAST III COSINUS project

MAST - III
Marine Science and Technology Programme

COSINUS

partially funded by the E.C., Directorate General XII under contract no. MAS3-CT97-0082.

COSINUSTaskA.1:TurbulenceDamping

Analysis of near-wall turbulence modelling with *k*-ε models

REPORT HYD/ET/00/COSINUS2

December 2000

Erik A. Toorman

Hydraulics Laboratory
K.U.Leuven

Acknowledgements

This work has been carried out within the framework of the post-doctoral research project, funded through the authors fellowship by the Fund for Scientific Research Flanders, and of the MAST3 COSINUS project, funded in part by the European Commission, Directorate General XII for Science, Research & Development under contract no. MAS3-97-0082.

The authors post-doctoral position has been financed by the Flemish Fund for Scientific Research (FWO Vlaanderen).

Analysis of near-wall turbulence modelling with *k*-ε models

1. INTRODUCTION

When applying the *k*-ε model to various flow problems, several problems are encountered due to the limitations of the model, which assumes isotropic turbulence. In this report an investigation is done about the laminarisation due to the damping of turbulence in regions near a solid wall, a density interface or a free surface. The major part of this study deals with near-wall turbulence damping and homogeneous (single-phase) fluids because this has been widely studied and various solution methods and/or damping closures have been proposed in the literature. Several of them are reviewed. Two modelling strategies are investigated: the low-Reynolds models which solve the *k*-ε turbulence model equations up to the wall using damping functions, and the two-layer approach, where the wall layer is solved with a modified Van Driest-like mixing-length model. Model results are evaluated against experimental and DNS data.

As lutocline formation goes together with strong damping of turbulence, the turbulent Reynolds number ($R_t = k^2/\nu\varepsilon$) becomes small and the standard *k*-ε model is no longer valid. Preliminary simulations with the KUL research code "FENST" resulted in eddy viscosities as low as 10^{-9} m^2/s near a lutocline and indicate convergence problems for the *k*-ε model for eddy viscosities smaller than the kinematic viscosity of the fluid (Toorman, 1998a), which is a sign for the invalidity of the standard *k*-ε model. Therefore, a study is undertaken of laminarisation (or low-Reynolds) effects and how to modify the turbulence model to account for it. As a first step, low-*Re* *k*-ε models, which have been developed primarily for near-wall turbulence, are reviewed in a literature study and validated with the code FENST. These models are based on semi-empirical correction factors (damping functions) for the various constants in the *k*-ε equations, which are a function of the wall distance and R_t. The wall-distance dependance makes them unsuitable to be applied to laminarised layers near a lutocline. Wall-distance independent formulations are very scarce in the literature and the few existing ones lack theoretical support and sufficient validation. Therefore, profiles of mean velocity, *k* and ε in the near-wall turbulent boundary layer and viscous sublayer are re-analysed. New damping functions are defined for each variable in terms of the ratio of the physical value to the theoretical value in fully developed turbulent flow. Combinations of these damping functions allows a more exact determination of the model damping functions f_μ, f_1 and f_2. At present, it is too early to know how these near-wall damping functions can be related to the sought damping functions for lutocline regions.

This report is written in the context of the research under Tasks A.1 (sediment-turbulence interaction) of the MAST III *COSINUS* project, where the formation of density interfaces (lutoclines) in turbulent flow of cohesive sediment suspensions is studied using the *k*-ε model.

2. BASIC EQUATIONS

Throughout this text, a homogeneous fluid with constant density and viscosity is considered.

2.1. TRANSPORT EQUATIONS FOR k AND ε

The turbulent kinetic energy (TKE) k is defined as (De Mulder, 1997, p.114):

$$k = \sum_i \frac{1}{2} \overline{u_i' u_i'} \qquad \textbf{(1)}$$

where: u'_i = fluctuation on velocity component i (= 1 - n, with n the dimension). The turbulent dissipation rate (TDR) ε is defined as (De Mulder, 1997, p.114):

$$\varepsilon = \sum_i \sum_j \nu \overline{\frac{\partial u_i'}{\partial x_j} \frac{\partial u_i'}{\partial x_j}} \qquad \textbf{(2)}$$

where: ν = the kinematic viscosity of the fluid.

The 2D equation for transport of turbulent kinetic energy is obtained by multiplying the Navier-Stokes equation with the velocity components u and v respectively, giving a transport equation for the Reynolds stress. Averaging, making a summation and dividing by two gives the exact form of the transport of k (e.g. Vandromme, 1993). In the Boussinesq approximation the turbulent stresses are described in analogy to the viscous stresses as (De Mulder, 1997, p.122):

$$\overline{u_i' u_j'} = -2\nu_t S_{ij} + \frac{2}{3} k \delta_{ij} \qquad \textbf{(3)}$$

where: S_{ij} = shear (or strain) rate tensor; ν_t = turbulent eddy viscosity, defined as a product of turbulence length and velocity scale (see further). The corresponding simplified form of the TKE equation then is:

$$\frac{\partial k}{\partial t} + U_i \frac{\partial k}{\partial x_j} = \frac{\partial}{\partial x_i} \left((\nu + \frac{\nu_t}{\sigma_k}) \frac{\partial k}{\partial x_i} \right) + P + G - \varepsilon \qquad \textbf{(4)}$$

An equation for the transport of ε is obtained by taking the derivative of the Navier-Stokes equations with respect to x_j, multiplying each side with $2\nu \partial u_i / \partial x_j$ and averaging (Launder, 1984). This formulation has been derived first by Davydov (1961). Its simplified form is:

$$\frac{\partial \varepsilon}{\partial t} + U_i \frac{\partial \varepsilon}{\partial x_j} = \frac{\partial}{\partial x_i} \left((\nu + \frac{\nu_t}{\sigma_\varepsilon}) \frac{\partial \varepsilon}{\partial x_i} \right) + \frac{f_1 c_1}{T_t} \left(P + (1 - c_3) G \right) - f_2 c_2 \frac{\varepsilon}{T_t} \qquad \textbf{(5)}$$

where: U_i = average flow velocity vector; T_t = turbulence time scale (see further); P = the shear production term:

$$P = \nu_t \left(\frac{\partial U_i}{\partial x_j} + \frac{\partial U_j}{\partial x_i} \right) \frac{\partial U_i}{\partial x_j} = \nu_t S_{II} \qquad \textbf{(6)}$$

where: S_{II} = shear rate intensity, the second invariant of the shear rate tensor, and G = the buoyancy term:

$$G = \frac{g}{\rho} \frac{\nu_t}{\sigma_t} \frac{\partial \rho}{\partial y} \qquad \textbf{(7)}$$

with σ_t = turbulent Schmidt number, the ratio of eddy viscosity to the turbulent mixing coefficient in the concentration transport equation, g = gravity constant, and f_1 and f_2 = low-Reynolds correction factors (see further). c_μ, c_1, c_2, σ_k and σ_ε are empirical constants. The most commonly used set of values of these constants is:

$$c_\mu = 0.09,\ c_1 = 1.44,\ c_2 = 1.92,\ \sigma_k = 1.0,\ \sigma_\varepsilon = 1.3$$

The derivation of the first three constants can be found in (Jakobsen, 1989) and (Chen & Jaw, 1998). The value of c_3 is still subject of debate. Rodi (1980) suggests to take a value in the range 0.8-1.0 for stable stratification. To extend the model to laminarisation effects (e.g. in the viscous sublayer near a wall), the model constants c_μ, c_1 and c_2 are multiplied by damping factors f_μ, f_1 and f_2 (see further).

> *Remark:* The previous derivation is strictly only valid for fluids with a constant density. As the k equation actually originate from the conservation of ρk, it is recommended that the given equation (4) would be compared to the following formulation where the diffusion is rewritten and an additional mass inertia term appears:
>
> $$\frac{\partial k}{\partial t} + U_i \frac{\partial k}{\partial x_j} + \frac{k}{\rho} \frac{d\rho}{dt} = \frac{1}{\rho} \frac{\partial}{\partial x_i} \left((\mu + \rho \frac{\nu_t}{\sigma_k}) \frac{\partial k}{\partial x_i} \right) + \nu_t \left(\frac{\partial U_i}{\partial x_j} + \frac{\partial U_j}{\partial x_i} \right) \frac{\partial U_i}{\partial x_j} + G - \varepsilon \qquad \textbf{(8)}$$
>
> The same remark applies to the conservation of ε.

2.2. TURBULENCE SCALES

Several parameters in turbulence modelling are based on scaling laws.

2.2.1. The k-ε turbulence scales

The k-ε scale is used to relate the mean-flow kinetic energy to the dissipation of kinetic energy in the larger eddies (Chen & Jaw, 1998). The corresponding time scale is:

$$T_t = k/\varepsilon \qquad \textbf{(9)}$$

Traditionally, the shear velocity u_* has often been used as velocity scale, particularly in low-Reynolds formulations (Patel et al., 1985). In order to avoid problems at a separation or

reattachment point where $u_* = 0$, it is convenient to replace u_* by $k^{1/2}$ (Lam & Bremhorst, 1981; Park & Sung, 1995). Kolmogorov (1942) and Prandtl (1945) had already independently proposed to use $k^{1/2}$ as velocity scale (Rodi, 1980).

A turbulence length scale L can be calculated as the product of turbulence velocity and time scale:

$$L = c_D \frac{k^{3/2}}{\varepsilon} \quad \textbf{(10)}$$

with: $c_D = c_\mu^{3/4} \cong 0.16$ (see further).

2.2.2. Kolmogorov scales

Kolmogorov (1941) found that the characteristics of small eddies are a function of ν and ε. These parameters can be used to define a second set of scales, the Kolmogorov microscales, introduced to relate the kinetic energy dissipation in the larger scales (ε) to the viscous dissipation in the smaller eddies (ν) (Chen & Jaw, 1998). The corresponding velocity scale is:

$$u_\varepsilon = (\nu\varepsilon)^{1/4} \quad \textbf{(11)}$$

the length scale η:

$$\eta = \frac{\nu^{3/4}}{\varepsilon^{1/4}} \quad \textbf{(12)}$$

and the time scale:

$$t = (\nu/\varepsilon)^{1/2} \quad \textbf{(13)}$$

2.2.3. Taylor microscale

The Taylor microscale (length scale) is defined as:

$$\lambda = \sqrt{\frac{\nu k}{\varepsilon}} \quad \textbf{(14)}$$

2.2.4. Turbulence Reynolds number

The turbulence Reynolds number R_t is the ratio of the product of the turbulence velocity and length scale to the fluid viscosity. It is commonly defined as:

$$R_t = \frac{k^2}{\nu\varepsilon} \quad \textbf{(15)}$$

which defines a Reynolds number independent on the wall distance. It could also be defined in function of the mixing length as:

$$R_t' = \frac{\sqrt{k}\ell}{\nu} \tag{16}$$

One could also define a turbulence Reynolds number as the ratio of the Reynolds stress to the viscous stress, which reduces to the ratio of the eddy viscosity to the kinematic viscosity:

$$\nu_t^+ = \frac{\nu_t}{\nu} \tag{17}$$

ν_t^+ is the non-dimensionalized eddy viscosity. This is in the line of the traditional definition of Reynolds numbers as ratios of forces. Therefore, the latter definition may be preferable.

2.3. EDDY VISCOSITY

A general approach to formulate the eddy viscosity is to define it in terms of turbulent scales. The turbulent eddy viscosity is proportional to a velocity scale and a length scale (Rodi, 1980). Using the Prandtl mixing length one obtains:

$$\nu_t = \ell^2 \left|\frac{\partial u}{\partial y}\right| \tag{18}$$

Using the Kolmogorov-Prandtl velocity scale $k^{1/2}$ gives:

$$\nu_t = c_\mu' \sqrt{k} L \tag{19}$$

Defining the turbulent length scale L as the product of the turbulent velocity scale $k^{1/2}$ and the turbulent time scale T_t, i.e. using eq.(9), and accounting for the damping correction in the viscous and transition regions (e.g. the viscous sublayer), the eddy viscosity can be written as:

$$\nu_t = f_\mu c_\mu \frac{k^2}{\varepsilon} \tag{20}$$

with: f_μ = the eddy viscosity damping function, and $c_\mu = c_\mu' c_D$. Consequently:

$$\nu_t^+ = \frac{\nu_t}{\nu} = f_\mu c_\mu R_t \tag{21}$$

2.4. REALISABLE TURBULENCE TIME SCALE

In reality, the time scale should increase from k/ε at high R_t to the Kolmogorov scale $C_\tau(\nu/\varepsilon)^{1/2}$ for very small R_t (« 1). A time scale fulfilling both conditions is called "realisable". The value of C_τ is determined as follows (Goldberg & Apsley, 1997). In the viscous sublayer the 1D steady-state transport equation of k reduces to $\nu\partial^2 k/\partial y^2 = \varepsilon$. Assuming ε to be constant, one finds by integration:

$$k = \frac{y^2}{2}\frac{\varepsilon}{\nu} = \frac{y^2}{\left(C_\tau\sqrt{\nu/\varepsilon}\right)^2} \qquad \textbf{(22)}$$

i.e., at the wall $C_\tau = \sqrt{2}$.

A realisable time scale can be defined as (Durbin, 1991; Goldberg & Apsley, 1997):

$$T_t = \frac{k}{\varepsilon}\max\left(1, C_\tau/\sqrt{R_t}\right) \qquad \textbf{(23)}$$

This time scale has the disadvantage of a discontinuous change of the gradient from the high R_t to the Kolmogorov scale.

Yang & Shih (1993) and Pattijn et al. (1997) propose to define the turbulent time scale as the superposition of the two scales:

$$T_t = \frac{k}{\varepsilon} + \sqrt{\frac{\nu}{\varepsilon}} \qquad \textbf{(24)}$$

However, this seems an inconsistent comparison of the turbulent and molecular viscosity. A new, more logical formulation is proposed here as follows:

$$T_t = \sqrt{\frac{\nu_t/f_\mu + \nu}{c_\mu\varepsilon}} = f_T\frac{k}{\varepsilon} \qquad \textbf{(25)}$$

where: f_T = the time scale realisability factor (or damping factor), defined as:

$$f_T = \frac{T_t}{k/\varepsilon} = \sqrt{1 + \frac{\nu\varepsilon}{c_\mu k^2}} = \sqrt{1 + \frac{1}{c_\mu R_t}} \qquad \textbf{(26)}$$

Division of ν_t by f_μ is carried out to obtain nonreciprocal definitions of each. Consequently, the eddy viscosity should be rewritten as:

$$\nu_t = f_\mu' c_\mu k T_t = f_T f_\mu' c_\mu \frac{k^2}{\varepsilon} \qquad \textbf{(27)}$$

and one finds that $f_\mu = f_T f_\mu'$, where f_μ' accounts for possible other effects, to be investigated. The non-dimensionalized time scale is obtained as:

$$T_t^+ = \frac{u_*^2 T_t}{\nu} \qquad \textbf{(28)}$$

Chen & Jaw (1998) propose a two-scale model where the turbulent time scale for dissipation through destruction of eddies, the Kolmogorov time scale is used in the ε-equation. This two-scale *k*-ε model yielded improved results for simple shear flow problems (more particularly turbulent wakes).

2.5. REALISABILITY

Pattijn et al. (1997) demonstrate that the standard k-ε model is not "realisable", which means that certain turbulent stresses could become negative, which is physically impossible. They present a simple way to prove this and propose a remedy.

Suppose the strain rate component $S_{11} = -S_{22}$ and the other components to be zero. The normal *Re*-stress then becomes:

$$\frac{\overline{u_1' u_1'}}{2k} = \frac{1}{3} - c_\mu \tau S_{11} \qquad \textbf{(29)}$$

For the constant value of c_μ in the standard k-ε model this can become zero when $\tau S_{11} > 3.7$. Physically the stress should always be positive and decrease with increasing strain rate. These conditions can be satisfied by redefining c_μ as:

$$c_\mu = \left(A + \frac{3}{2} \tau S_{II} \right)^{-1} \qquad \textbf{(30)}$$

The value of A is found from the tuning test case for the standard k-ε model of fully-developed channel flow, for which $\tau S_{II} \approx 3.3$. One finds that $A = 6$ to obtain $c_\mu = 0.09$.

3. NEAR-WALL EFFECTS

This section investigates the behaviour of various parameters for turbulent shear flow of a homogeneous fluid (i.e. with constant density and viscosity) in the vicinity of the wall. We consider the case of steady uniform (fully-developed) turbulent open-channel flow, driven by a known pressure gradient $p' = \mathrm{d}p/\mathrm{d}x$. All other gradients in the x-direction are zero, as well as the average vertical velocity component. Consequently, there is no advection and the problem is quasi 1-dimensional.

We introduce here the non-dimensionalized velocity, defined as:

$$u_+ = u/u_* \tag{31}$$

with u_* the shear velocity defined by:

$$u_* = \sqrt{\tau_w/\rho} = \sqrt{\nu \left.\frac{\partial u}{\partial y}\right|_{y=0}} \tag{32}$$

where: τ_w = wall shear stress, and y = vertical coordinate (i.e. the distance from the wall). The wall distance is non-dimensionalized with $y_* = \nu/u_*$, giving:

$$y_+ = \frac{y u_*}{\nu} \tag{33}$$

The corresponding k-ε transport equations (eqs. 4 & 5) for open-channel flow can then be rewritten as:

$$\frac{\mathrm{d}}{\mathrm{d}y_+}\left(\left(1+\nu_t^+/\sigma_k\right)\frac{\mathrm{d}k_+}{\mathrm{d}y_+}\right) + \nu_t^+\left(\frac{\mathrm{d}u_+}{\mathrm{d}y_+}\right)^2 = \varepsilon_+ \tag{34}$$

$$\frac{\mathrm{d}}{\mathrm{d}y_+}\left(\left(1+\nu_t^+/\sigma_\varepsilon\right)\frac{\mathrm{d}\varepsilon_+}{\mathrm{d}y_+}\right) + \frac{f_1 c_1 \nu_t^+}{T_t^+}\left(\frac{\mathrm{d}u_+}{\mathrm{d}y_+}\right)^2 = \frac{f_2 c_2 \varepsilon_+}{T_t^+} \tag{35}$$

The near-wall distributions are discussed based on various experimental data and DNS data for closed channel flow from Kim *et al.* (1987) and Kim (1989), a developing turbulent boundary layer from Spalart (1988)[1] and open-channel flow (Knowlton, pers. comm., 1999). The DNS data must be interpreted carefully as they are not exact solutions due to the limitations of DNS (e.g. restricted to relatively low global Reynolds numbers).

---

[1] These DNS data are available from the *"Collaborative Testing of Turbulence Models"* data bank (*Bradshaw et al.*, 1996), accessible through the *Journal of Fluids Engineering* web pages at the URL: http://scholar.lib.vt.edu/ejournals/JFE/data/JFE/DB96-243/d4/simul1.dat.

3.1. STRESS DISTRIBUTION

In the case of fully-developed turbulent open-channel flow the *x*-momentum equation reduces to:

$$-\frac{\partial p}{\partial x} + \frac{\partial \tau}{\partial y} = 0 \qquad \textbf{(36)}$$

where: τ = total stress, which is given by:

$$\tau = \tau_{Re} + \tau_{\mu} = -\rho\,\overline{u'v'} + \mu\frac{\partial u}{\partial y} = \rho\left(\nu_t + \nu\right)\frac{\partial u}{\partial y} \qquad \textbf{(37)}$$

with: τ_{Re} = Reynolds stress, and τ_{μ} = viscous stress. In non-dimensional form:

$$\tau_+ = \frac{\tau}{\rho u_*^2} = -\overline{u'v'}_+ + \frac{\partial u_+}{\partial y_+} = \left(1 + \nu_t^+\right)\frac{\partial u_+}{\partial y_+} \qquad \textbf{(38)}$$

The total stress distribution over the water column is easily obtained by integration between the bottom and a distance *y*:

$$\tau_w = -\frac{\mathrm{d}p}{\mathrm{d}x}\,y + \tau(y) \qquad \textbf{(39)}$$

Equivalently, integration between a certain *y* and the free surface, where $\tau(H) = 0$, yields:

$$\tau(y) = -\frac{\mathrm{d}p}{\mathrm{d}x}\,(H - y) = -\frac{\mathrm{d}p}{\mathrm{d}x}\,H\,(1 - \eta) \qquad \textbf{(40)}$$

where: H = water depth, $\eta = y/H$. Consequently, since $\tau(0) = \tau_w$, the pressure gradient is related to the bottom shear stress by:

$$\frac{\mathrm{d}p}{\mathrm{d}x} = -\frac{\tau_w}{H} \qquad \textbf{(41)}$$

The pressure gradient can be non-dimensionalized as:

$$p_+' = \frac{y_*}{\rho u_*^2}\frac{\mathrm{d}p}{\mathrm{d}x} = -\frac{1}{H_+} \qquad \textbf{(42)}$$

The stress distribution, eq.(38) or (39), in non-dimensional form reads:

$$\tau_+ = 1 - \eta \qquad \textbf{(43)}$$

The traditional approximation that the total stress near the wall is constant then is only strictly valid when there is no pressure gradient. If we consider only a wall layer of thickness δ, such that $\delta/H \ll 1$, the total stress can be considered approximately constant in this thin layer as the

pressure gradient contribution can be neglected and thus $\tau_+ \cong 1$.

From equations (38) and (43) it follows that the viscous stress can be written as:

$$\frac{\partial u_+}{\partial y_+} = \frac{1-\eta}{1+\nu_t^+} \tag{44}$$

and, hence, the Reynolds stress:

$$-\overline{u'v'}_+ = 1-\eta-\frac{\partial u_+}{\partial y_+} = \frac{\nu_t^+(1-\eta)}{1+\nu_t^+} \tag{45}$$

The ratio of turbulent Reynolds stress to the viscous stress naturally yields the eddy viscosity:

$$\frac{-\overline{u'v'}_+}{\dfrac{\partial u_+}{\partial y_+}} = \nu_t^+ \tag{46}$$

and defines a turbulent Reynolds number (see Section 2.2.3).

The distribution of the stresses in the near wall region is shown in figure 1 and seems to be well described by the analytical function, derived from the modified Van Driest hypothesis (see Section 3.2). Comparison with experimental data shows that these relationships are indeed a good approximation. At the wall, the Reynolds stress varies with $(\alpha y_+)^3$ (Patel *et al.*, 1985), as is confirmed by DNS data (Hwang & Lin, 1998). The decrease of the Reynolds stress for higher y_+ in most of the DNS data is due to the thinness of the turbulent layer in the cases considered (related to the limitations of DNS at higher Reynolds numbers).

3.2. EDDY VISCOSITY AND MIXING LENGTH DISTRIBUTION

Assuming a logarithmic velocity profile and a molecular viscosity negligibly small compared to the eddy viscosity, one finds the well-known parabolic eddy viscosity profile for open-channel flow:

$$\nu_t = \frac{\tau}{\rho\dfrac{\partial u}{\partial y}} = \frac{u_*^2(1-\eta)}{\dfrac{u_*}{\kappa y}} = \kappa u_* y(1-\eta) \tag{47}$$

The corresponding Prandtl mixing length, following eq.(18), is given by:

$$\ell = \sqrt{\frac{\nu_t}{\dfrac{\partial u}{\partial y}}} = \kappa y\sqrt{1-\eta} \tag{48}$$

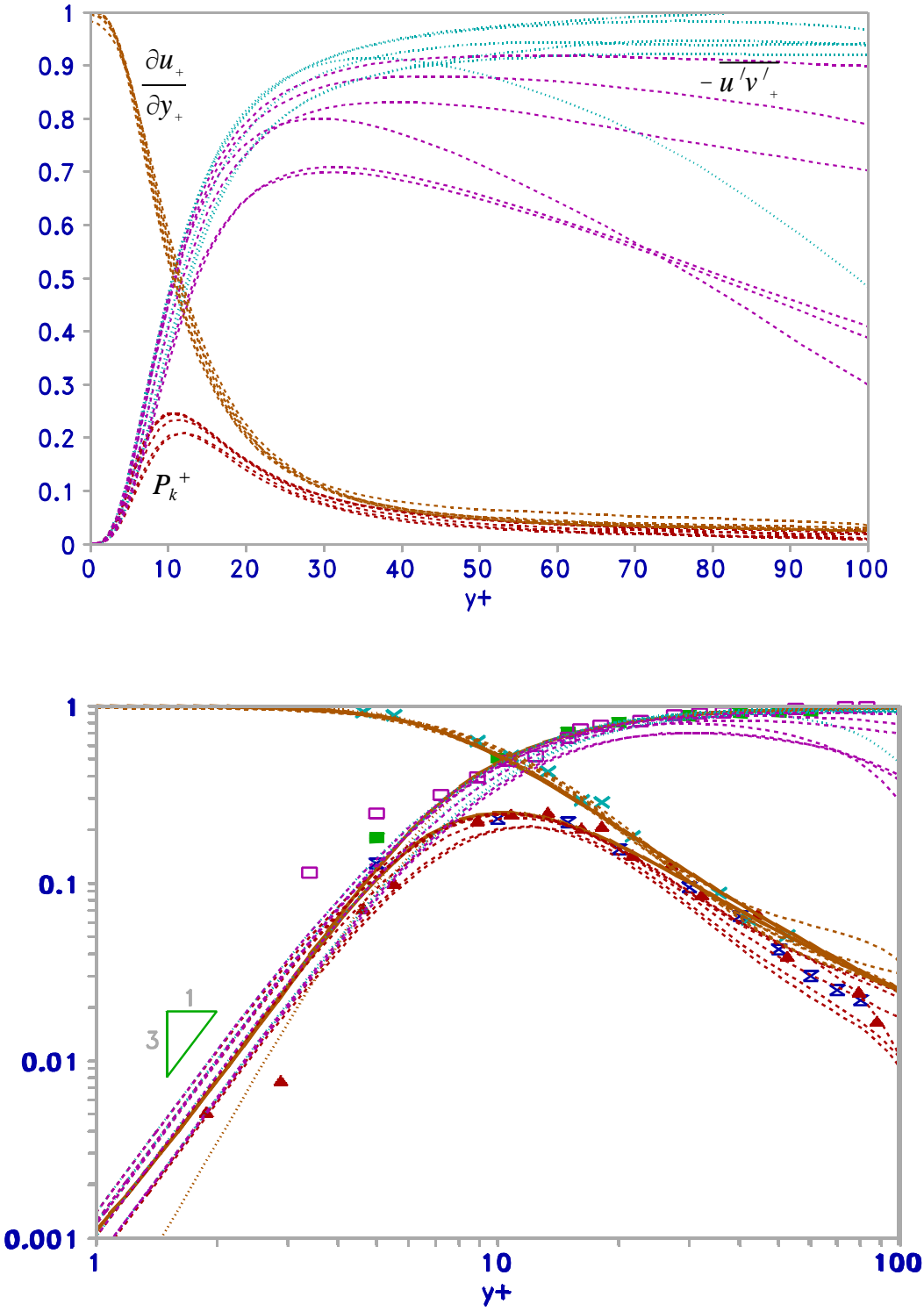

Figure 1: Near-wall distribution of the non-dimensionalized Reynolds stress, viscous stress (du_+/dy_+) and TKE production (P_k^+). Dotted lines in bottom figure = original Van Driest distribution; full lines = modified Van Driest distribution; dashed lines = DNS data; symbols = experimental data (□ = Schubauer, 1954; digitized from figure 1 in Patel *et al.*, 1985; ■ and ⧖ = Kim *et al.*, 1968; digitized from Fig.9 in Spalart, 1988; × and ▲ = Laufer, 1954); dotted lines in upper figure = $\tau_{Re}/(1-\eta)$.

In reality, the eddy viscosity profile in open-channel flow is not exactly parabolic due to deviations at the wall and at the free surface. Van Driest (1956) introduced an empirical damping factor f_ℓ to extend the validity of eq.(48) to the viscous sublayer and the transition layer:

$$\ell = f_\ell \kappa y \sqrt{1-\eta} \tag{49}$$

where f_ℓ = the mixing length damping function:

$$f_\ell = 1 - e^{-y_+/A_+} \tag{50}$$

with: A_+ a damping constant (= 26.0 for smooth walls).

However, the original Van Driest damping function results in a near-wall variation of the Reynolds stress with y_+^4 instead of y_+^3 (fig.1). In order to fulfil the latter condition the damping function can be modified as follows:

$$f_\ell = 1 - \exp\left(-(y_+/A_+)^{\frac{1/2+y_+}{1+y_+}} \right) \tag{51}$$

where A_+ retains the same value as before. This modification results in the correct asymptotic behaviour at the wall (fig.1). According to this modified damping function, the mixing length at the wall varies according $\alpha y_+^{3/2}$.

Exact relationships can be derived as follows. The near-wall stress balance, eq.(37), can be rewritten in terms of the mixing length as:

$$\frac{\tau_w}{\rho} = u_*^2 = \ell^2 \left(\frac{du}{dy} \right)^2 + \nu \frac{du}{dy} - \frac{y}{\rho} \frac{dp}{dx} \tag{52}$$

Replacing the velocity gradient with ν_t / ℓ^2 gives a quadratic equation in the eddy viscosity, which solution (in non-dimensionalized form) is given by:

$$\nu_t^+ = \frac{-1 + \sqrt{1 + 4\ell_+^2 (1 + yp'/\tau_w)}}{2} \tag{53}$$

where the mixing length is non-dimensionalized with y_*. For open-channel flow it can be rewritten as:

$$\nu_t^+ = \frac{-1 + \sqrt{1 + 4\ell_+^2 (1-\eta)}}{2} \tag{54}$$

Equation (54) can be inverted to give the mixing length expressed in terms of the relative eddy viscosity:

$$\ell_+ \sqrt{1-\eta} = \nu_t^+ \sqrt{1 + 1/\nu_t^+} \tag{55}$$

The non-dimensionalized velocity gradient (or viscous stress) becomes:

$$\frac{du_+}{dy_+} = \frac{\nu_t^+}{\ell_+^2} = \frac{-1+\sqrt{1+4\ell_+^2(1-\eta)}}{2\ell_+^2} \qquad \textbf{(56)}$$

Hence, provided that the velocity distribution is known (or the eddy viscosity or mixing length distribution), the profiles of the other variables can be reconstructed using the equations (44)-(46) and (54)-(56).

Notice that the general relationships between stresses, eddy viscosity and mixing length are valid for any fully-developed (!) open-channel flow, thus also sediment-laden flows. Hence, the measurement of a velocity profile allows the determination the eddy viscosity profile, provided that the shear velocity is well known. In practice it is not easy to accurately determine the shear velocity experimentally.

The mixing length damping function for fully-developed open-channel flow can be defined from substituting the mixing length definition in the equality:

$$\frac{\tau}{\rho} = u_*^2(1-\eta) = (\nu+\nu_t)\frac{du}{dy} \qquad \textbf{(57)}$$

which results in:

$$\ell = \frac{u_*\sqrt{1-\eta}}{\frac{du}{dy}}\sqrt{1-\frac{\nu\frac{du}{dy}}{u_*^2(1-\eta)}} \qquad \textbf{(58)}$$

Hence:

$$f_\ell = \frac{u_*}{\kappa y\frac{du}{dy}}\sqrt{1-\frac{\nu\frac{du}{dy}}{u_*^2(1-\eta)}} = \frac{1}{\kappa y_+\frac{du_+}{dy_+}}\sqrt{1-\frac{1}{1-\eta}\frac{du_+}{dy_+}} \qquad \textbf{(59)}$$

which defines the mixing length damping function in terms of the velocity gradient and the shear velocity.

Data processing shows that the turbulent length scale L, defined by eq.(10) or (18), has another distribution than the Prandtl mixing length ℓ (figure 3). The distribution of the eddy viscosity and the turbulence length scales in the outer region of the wall layer (where $\eta \ll 1$) is given by:

$$\nu_t^+ = \ell_+ = \kappa y_+ \qquad (y_+ \gg 1,\ \eta \ll 1) \qquad \textbf{(60)}$$

which is also clearly seen in figure 3. It is also noticed that the "real" maximum eddy viscosity, as computed with the low-R_t model, is smaller than that of the parabolic profile, which is typical for a k-ε model. The near-wall profiles of the ratio of the non-dimensional eddy viscosity to its outer-region variation ($f_\nu = \nu_t^+/\kappa y_+$) are shown in figure 4. It can be noticed that the Van Driest hypothesis does not reach the asymptotic line as fast.

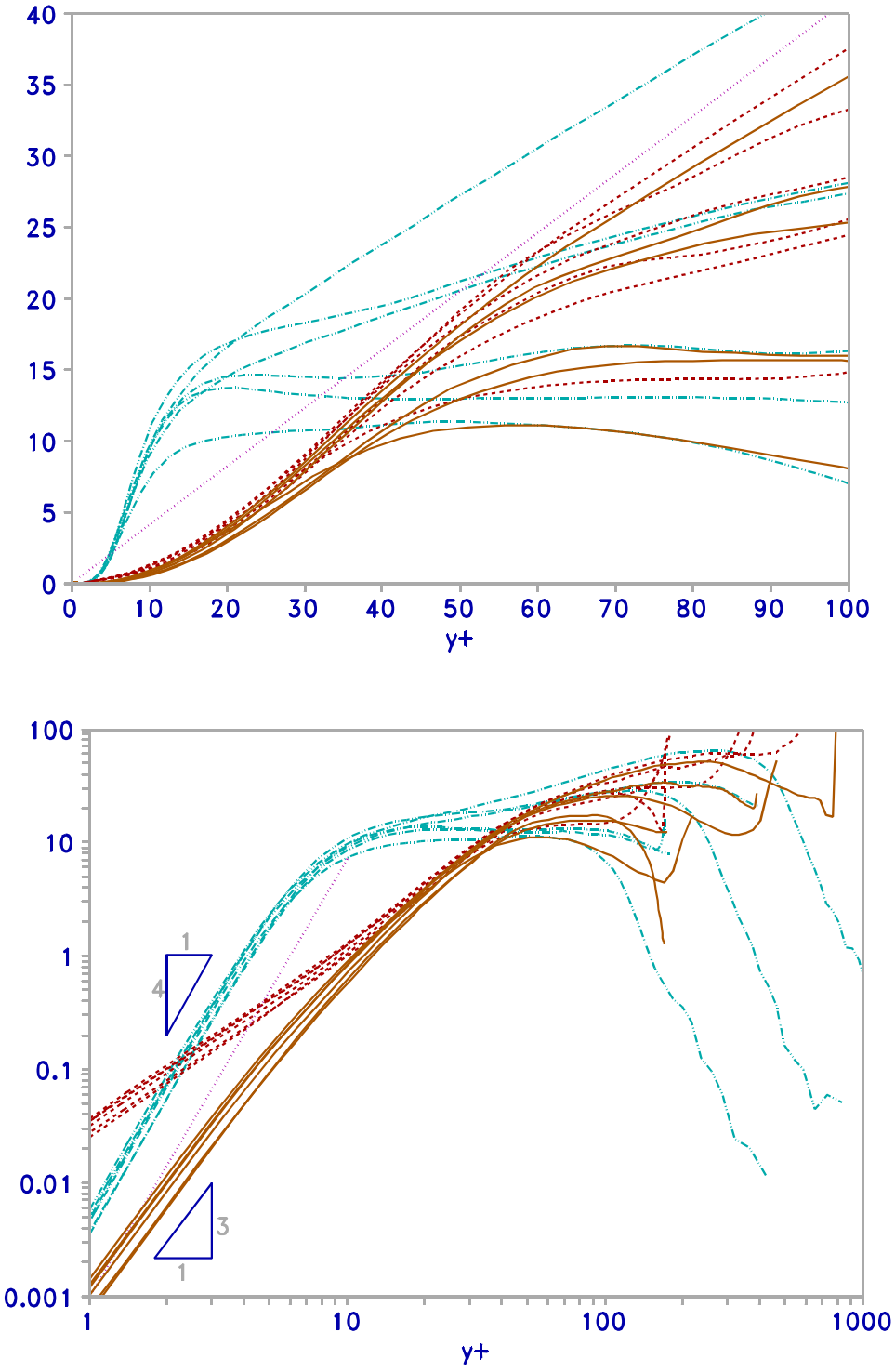

Figure 2: Distribution of non-dimensional eddy viscosity (ν_t^+ = full lines), Prandtle mixing length (ℓ_+ = dashed lines) and turbulent Reynolds number ($c_\mu R_t$ = centred lines) derived from DNS data. Dotted line = κy_+, the asymptotic behaviour in the ideal log-layer.

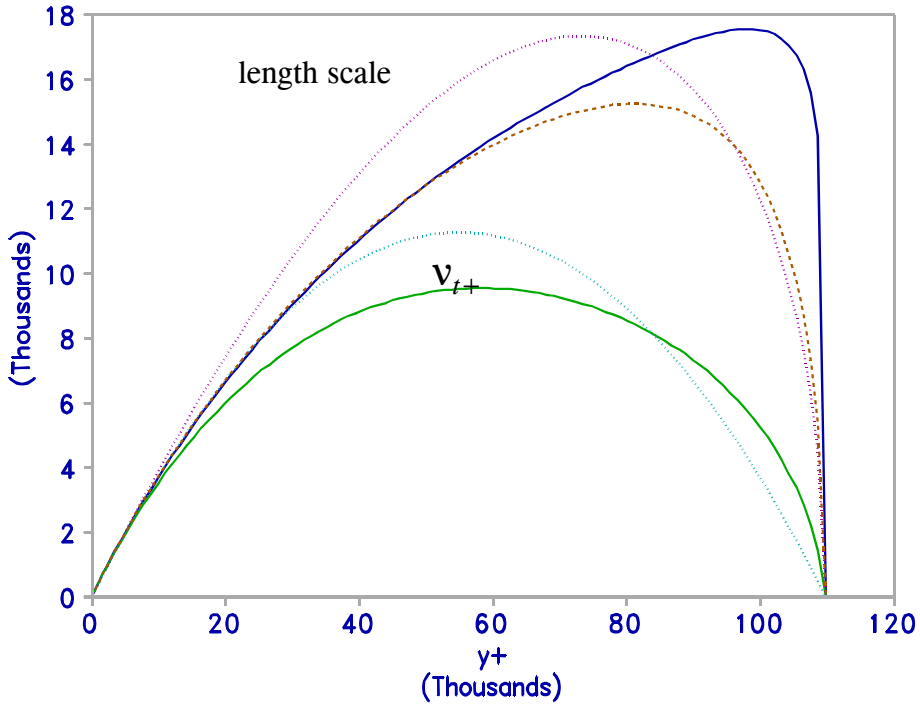

Figure 3: Distribution of non-dimensional turbulence length scale and eddy viscosity in open-channel flow. Full line = low-R_t calculation and corresponding Prandle mixing length ℓ_+; dashed line = corresponding L_+; dotted line = Van Driest and ideal parabolic eddy viscosity distribution and corresponding ℓ_+.

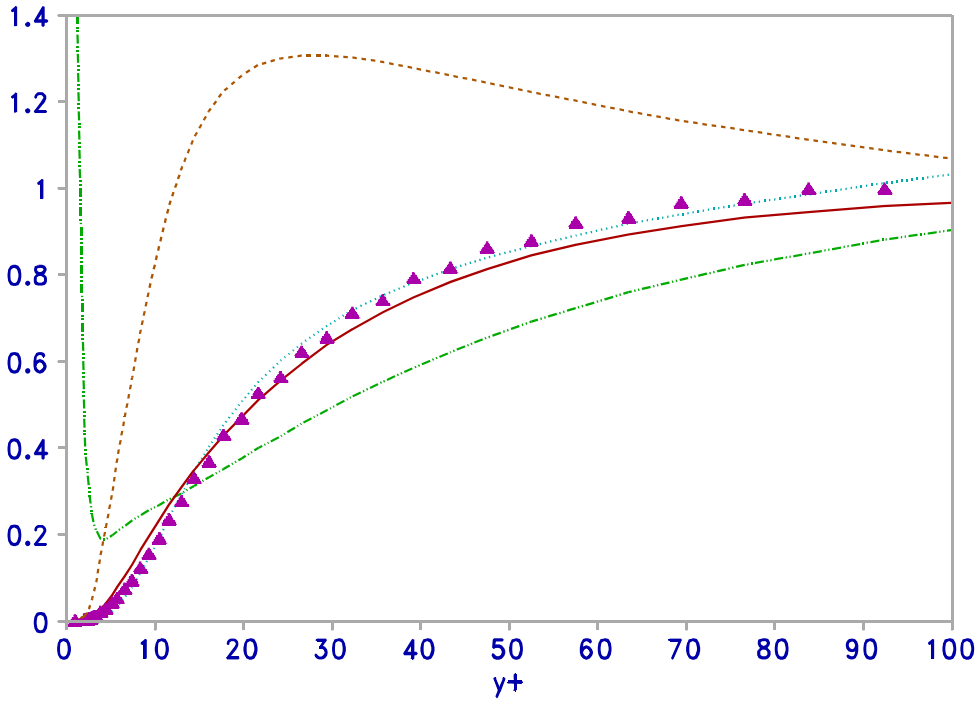

Figure 4: Near-wall distribution of $\nu_t^+/\kappa y_+$. Full line = from Van Driest hypothesis; dotted line = approximation (from eq.54); ▲ = FENST-2D low-Reynolds simulation; dashed line = $c_\mu k_+^2/\varepsilon_+\kappa y_+$; centred line = f_μ = $\nu_t^+/(c_\mu k_+^2/\varepsilon_+)$.

3.3. TKE PRODUCTION DISTRIBUTION

The exact distribution of the production of turbulent kinetic energy in fully-developed open-channel flow can be calculated as:

$$P_k^+ = P_k \frac{\nu}{u_*^4} = -\overline{u'v'}_+ \frac{\partial u_+}{\partial y_+} = \nu_t^+ \left(\frac{1-\eta}{1+\nu_t^+} \right)^2 \qquad \textbf{(61)}$$

The profile corresponding to the Van Driest hypothesis, compared with experimental data, is shown in figure 1. It is noticed through DNS that the profiles of P_k seem to be little dependent on the Reynolds number and correspond well with experimental data (Spalart, 1988). In the fully developed region, it behaves asymptotically as $1/\kappa y_+$. It can be noticed that the P_k^+ data obtained with DNS lies systematically lower than the viscous diffusion (figure 1). Equation (61) inversed gives:

$$\nu_t^+ = \frac{1-\eta+\sqrt{(1-\eta)\,(1-\eta-4P_k^+)}}{2P_k^+} - 1 \qquad \textbf{(62)}$$

These equations show that P_k^+ reaches a maximum value of 0.25 in the inner near-wall layer ($\eta \ll 1$) where $\nu_t^+ = 1$ or $\nu_t = \nu$.

3.4. TURBULENT KINETIC ENERGY DISTRIBUTION

The turbulent kinetic energy (TKE) is non-dimensionalized as:

$$k_+ = k/u_*^2 \qquad \textbf{(63)}$$

Its distribution is shown in figure 5. At the wall k_+ varies with y_+^2 with a proportionality coefficient of 0.025 - 0.05, depending on Re_T (Patel *et al.*, 1985). This has been confirmed by DNS data (Hwang & Lin, 1998). It is found experimentally that in the fully turbulent region its value is of the order of $c_\mu^{-1/2}$ (= 10/3). From averaging experimental data Patel *et al.* (1985) conclude that k_+ may be even constant (= $c_\mu^{-1/2}$) over a certain range of y_+. DNS data (Hwang & Lin, 1998) and low-Reynolds k-ε model results (see further) clearly show that this is not the case. Moreover, the DNS data show that the k_+ profile varies with the Reynolds number (Hwang & Lin, 1998).

The turbulent kinetic energy can be related to the turbulence length scale L by the Kolmogorov-Prandtl relationship, eq.(19). This yields an identical distribution as for the Reynolds stress, provided that $c_\mu' = c_\mu^{1/4} \cong 0.54$. Comparison with data shows that this relationship is invalid in the inner near-wall region.

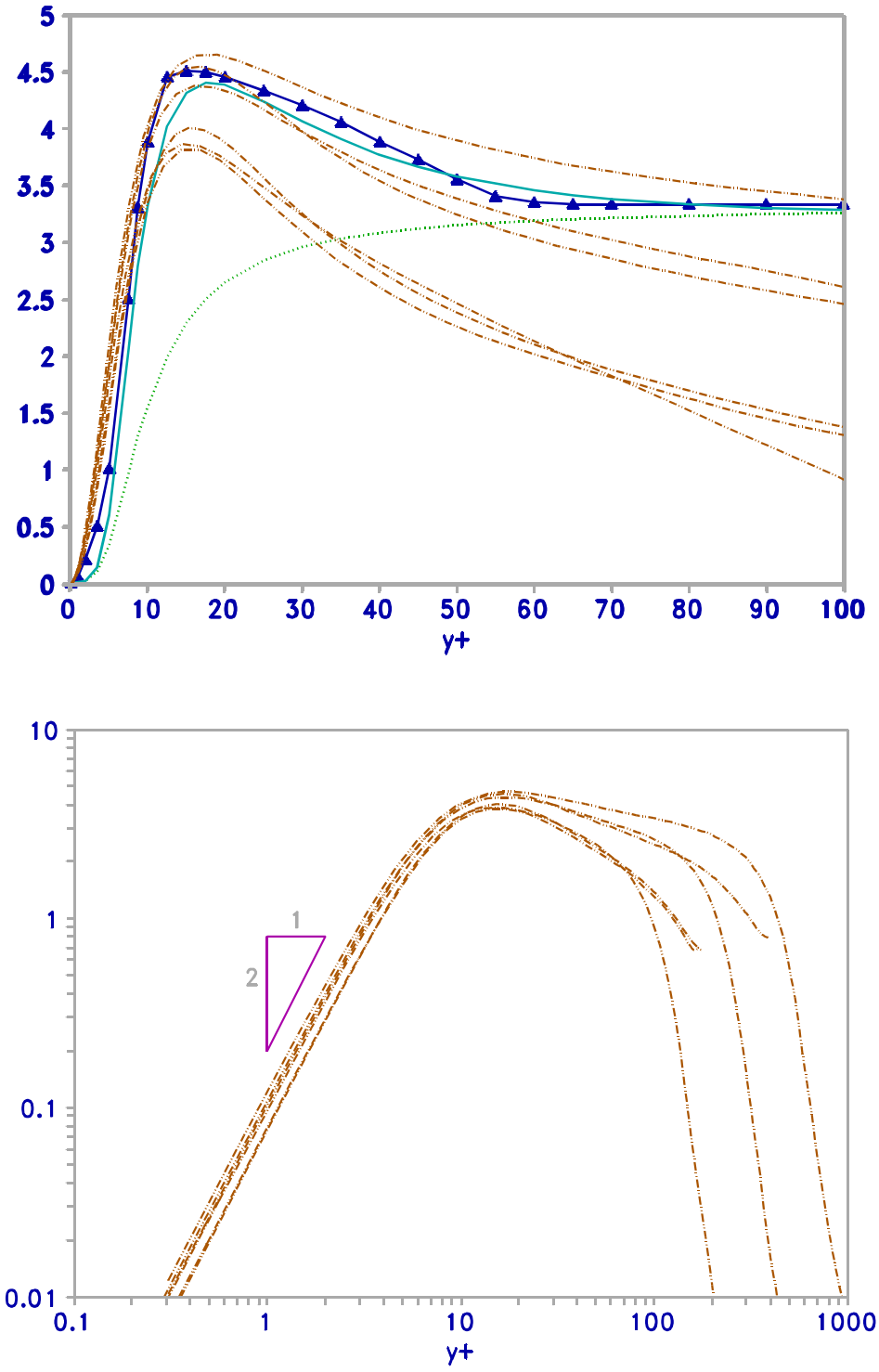

Figure 5: Near-wall distribution of non-dimensionalized turbulent kinetic energy k_+. Full line = low-Reynolds model numerical solution (FENST-2D solution for Comte-Bellot experiment simulation with modified Lam-Bremhorst damping functions); –▲– = suggested average profile for various experimental data, proposed by Patel *et al.* (1985) (the uncertainty is of the order of 30%); dotted line = Prandtl-Kolmogorov distribution; centred lines = DNS simulations.

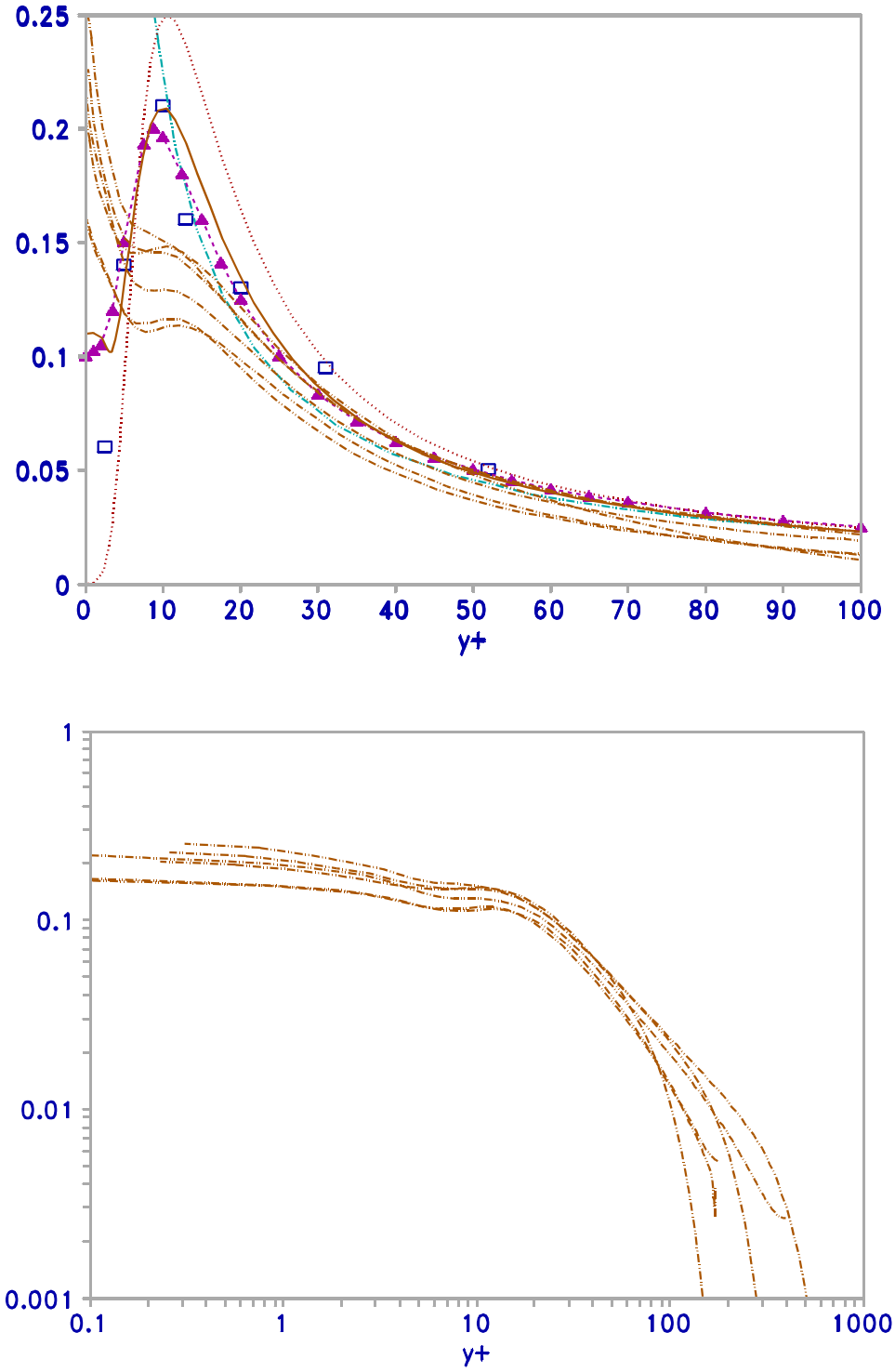

Figure 6: Near-wall distribution of the non-dimensional dissipation rate ε_+. Full line = low-Reynolds model numerical solution (FENST-2D solution for Comte-Bellot experiment simulation); –▲– = suggested average profile for various experimental data, proposed by Patel *et al.* (1985) (the uncertainty for $y_+ < 30$ is $>40\%$ with a maximum of nearly 100% around $y_+ = 10$); dotted line = Prandtl-Kolmogorov distribution ($\varepsilon_+ = P_k^+$); centred line = asymptotic behaviour (eq.65), □ = experimental data (Laufer, 1954); centred lines = DNS data.

3.5. DISSIPATION RATE DISTRIBUTION

The turbulent dissipation rate is non-dimensionalized as:

$$\varepsilon_+ = \frac{\nu\varepsilon}{u_*^4} \tag{64}$$

Distributions of ε_+ according to various methods are shown in figure 6. In the fully turbulent region its asymptotic behaviour is:

$$\lim_{y_+ \to \infty} \varepsilon_+ = 1/\kappa y_+ \tag{65}$$

According to the review by Patel *et al.* (1985), experimental data indicate a finite value at the wall in the range 0.05-0.10, with the highest value for higher Reynolds numbers. The exact value at the wall is found from the *k*-equation, giving:

$$\varepsilon_{(y=0)} = \nu \frac{\partial^2 k}{\partial y^2}_{(y=0)} \tag{66}$$

As the near-wall distribution of k is proportional to y^2 (see Section 3.4), ε tends to a constant value at the wall, i.e. a zero-gradient boundary condition can be employed as well (Patel *et al.*, 1985):

$$\frac{\partial \varepsilon}{\partial y}_{(y=0)} = 0 \tag{67}$$

Numerical simulations with low-*Re* models by the author indeed show no significant difference between these two wall boundary conditions. In practice, the zero-gradient BC proves to yield better convergence.

An estimate of the turbulent dissipation rate can be calculated with eq.(10). When the Prandle mixing length is used as length scale, this gives exactly the same profile as for P_k^+, which implies that the Kolmogorov-Prandtl scaling implicitly assumes equilibrium over the entire boundary layer, which is incorrect for the inner layer.

The dissipation rate can also be calculated from the k equation by numerical differentiation using the k-profile data. In non-dimensional form, the k equation for a fully developed turbulent boundary layer reads:

$$\varepsilon_+ = \frac{\partial}{\partial y_+}\left((1 + \nu_t^+) \frac{\partial k_+}{\partial y_+} \right) + P_k^+$$

The original data, digitized from Patel *et al.* (1985) show some important deviations. By trial and error the values can be modified to obtain much better agreement with averaged ε profile from Patel *et al.* (1985). This optimized result supports the empirical indication that ε at the wall is not zero. Of course one has to bear in mind that the suggested averaged profile can be just as much erroneous as the initial k profile. Nevertheless the obtained k profile is much more in agreement with DNS data (Spalart, 1988) than the averaged curve of Patel *et al.*

DNS data show a short plateau (or local maximum) around $y_+ = 10$ and then an increase towards the wall (Spalart, 1988; So *et al.*, 1996). This can be accounted for in low-*Re* models by including a pressure diffusion term (Hwang & Lin, 1998). The data from Knowlton (1999)

show a significant difference between the directly computed value of ε_+ and the one obtained from making the sum of production and diffusion of TKE. This clearly demonstrates that DNS data must be interpreted with care and that they should not be considered as exact.

3.6. PRODUCTION-DISSIPATION BALANCE

The near-wall distribution of the ratio of production to the dissipation of turbulent kinetic energy:

$$\frac{P_k}{\varepsilon} = \frac{P_k^+}{\varepsilon_+} \tag{69}$$

is shown in figure 7. Due to the narrow shear layer thickness (low Reynolds number cases) the DNS data do not allow to determine over which width the assumption $P_k/\varepsilon \approx 1$ is valid. It may be noticed that the distribution of P_k/ε is very similar to that of $c_\mu^{-1/2} k_+$, but the maximum is reached at another y_+.

3.7. TKE BALANCE

DNS allows the calculation of the various terms in the exact *TKE* balance equation (for a constant density fluid) (e.g. Chen & Jaw, 1998):

$$\frac{\mathrm{D}k}{\mathrm{D}t} = \frac{\partial}{\partial x_i}\left(\nu \frac{\partial k}{\partial x_i} - \frac{\overline{u_j' u_j' u_i'}}{2} - \frac{\overline{p' u_i'}}{\rho} \right) - \overline{u' v'} \frac{\partial U_i}{\partial x_j} - \varepsilon \tag{70}$$

The contributions, as obtained for steady state open-channel test case ($\mathrm{D}k/\mathrm{D}t = 0$), are shown in figure 8. The sum is not exactly zero, giving a measure of the error of DNS calculations.

Notice that the viscous and turbulent diffusion are negative over a thin layer near $y_+ = 10$. The shear production is maximal where viscous and turbulent diffusion are negative and equal. The maximum dissipation rate at the wall is the result of viscous dissipation.

Remark: In the simplified k-ε model, turbulent and pressure diffusion are taken together and replaced by the eddy diffusion term (Boussinesq approximation).

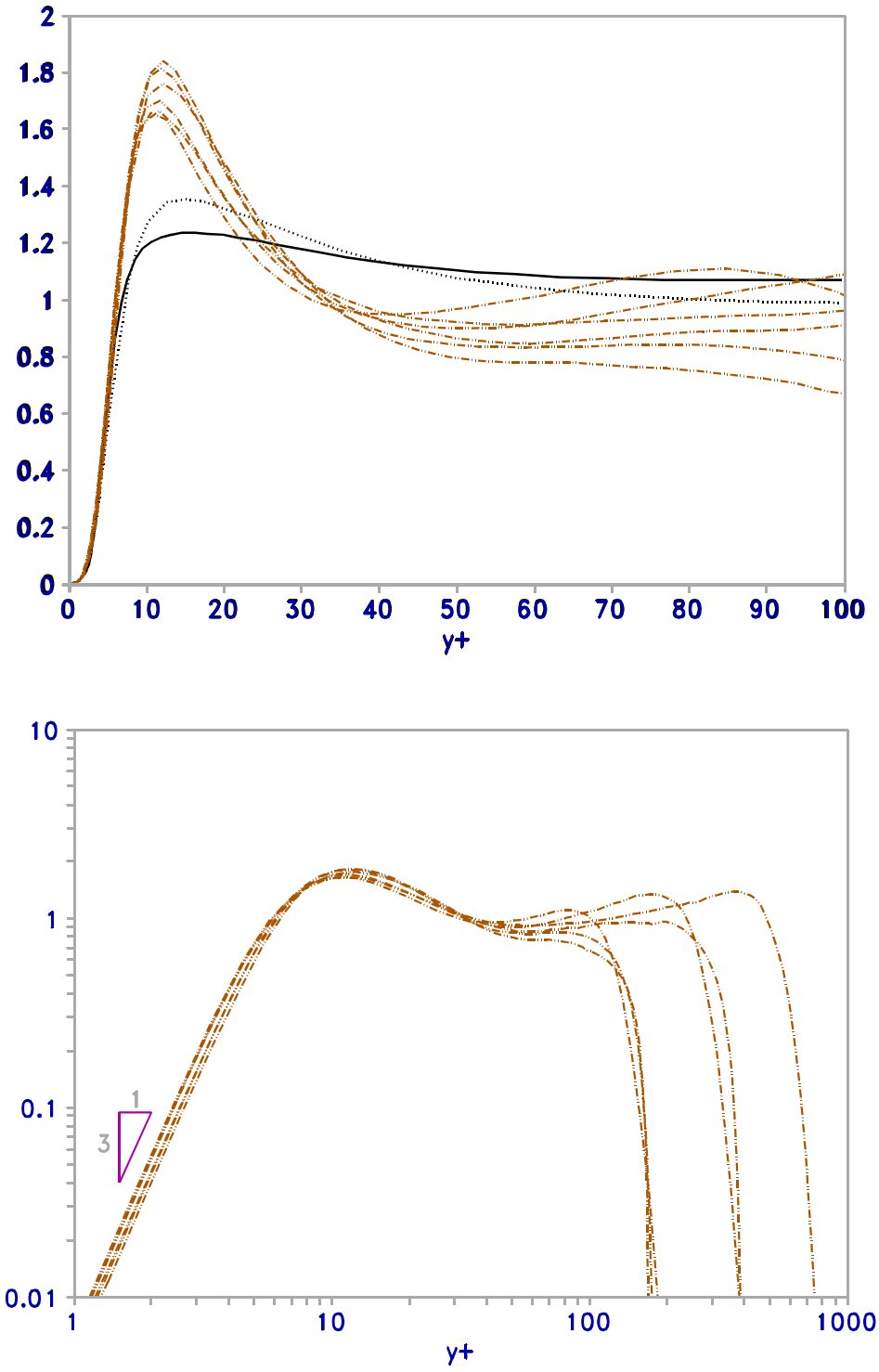

Figure 7: Near-wall distribution of P_k/ε. Full line = low-Reynolds model result (FENST-2D solution for Comte-Bellot experiment simulation); dotted line = averaged data (Patel *et al.*, 1985); centred lines = DNS data.

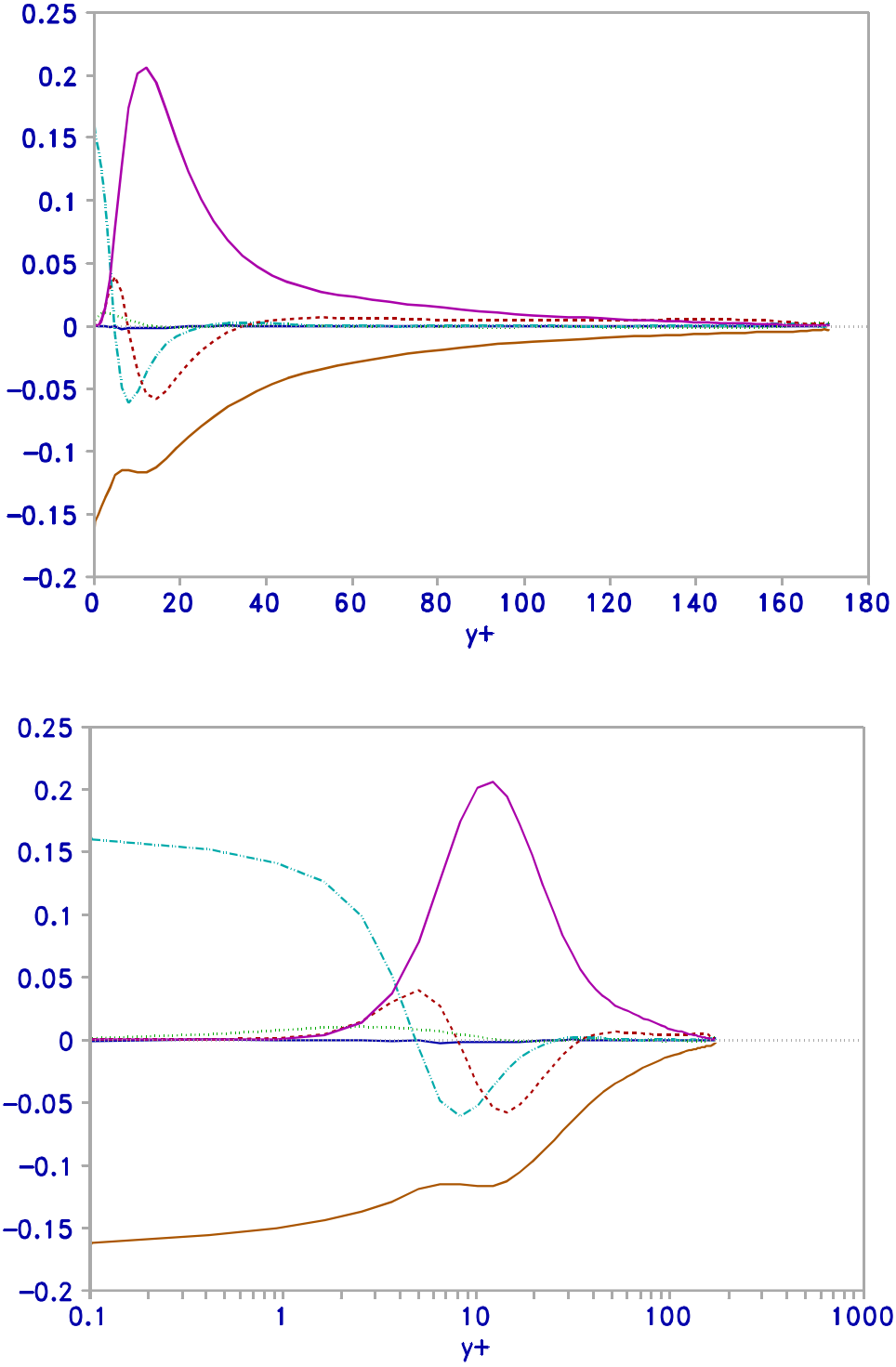

Figure 8: TKE budget for fully-developed turbulent open channel flow (DNS data from Knowlton, 1999). Distribution of production (upper full line), dissipation (lower full line), viscous diffusion (centred line), turbulent diffusion (dashed line) and pressure diffusion (dotted line).

3.8. VELOCITY DISTRIBUTION

3.8.1. The standard Law-of-the-Wall

As the velocity at the wall is zero, there is a thin viscous sublayer adjacent to the wall. The simple laminar Newtonian velocity profile under uniform shear reads:

$$u = \frac{\tau_w}{\mu} y \qquad \textbf{(71)}$$

The non-dimensional velocity profile in the viscous sublayer then becomes:

$$u_+ = y_+ \qquad \textbf{(72)}$$

where: $y_+ = y/y_*$, the non-dimensionalized distance from the wall, with $y_* = \nu/u_*$, where ν = (molecular) kinematic viscosity of the fluid = μ/ρ. This corresponds well with experimental data up to a certain distance Y_+ from the wall, which depends on the friction characteristics (Fig.1).

Away from the wall, in the fully turbulent region, the velocity profile can be well fitted with a logarithmic law (figure 9), as was first proposed by Nikuradse (1932):

$$u_+ = \frac{1}{\kappa}\ln(y/y_0) \qquad (y_+ > Y_+) \qquad \textbf{(73)}$$

where y_0 = the equivalent roughness height.

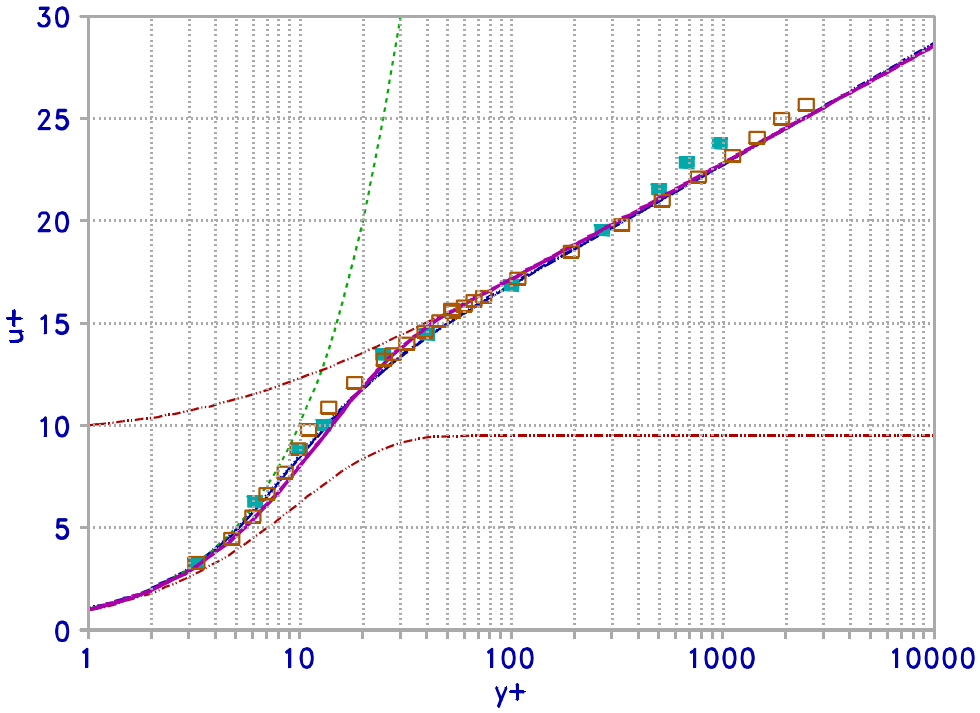

Figure 9: Non-dimensional wall profile. Experimental data: ■ = Laufer (1954), □ = Comte-Bellot (1963). Dashed line = law of the wall; full line = continuous law of the wall; heavy dashed line = Van Driest (1956) numerically integrated.

The velocity profile which corresponds with the Van Driest mixing length distribution can be reproduced by numerical integration. This compares quite well with experimental data (figure 9).

3.8.2. Equivalent roughness height

The equivalent roughness height is often expressed in terms of a parameter E for smooth walls or the effective roughness height k_s, which is a function of the type of roughness element, its density and its mobility. For a smooth surface Nikuradse (1932) found empirically:

$$u_+ = \frac{1}{\kappa} \ln(E y_+) \qquad \textbf{(74)}$$

with: E = smooth wall roughness parameter (which has a value of about 9 $\pm$2). For a rough surface of glued uniform sand particles Nikuradse (1932) found empirically:

$$u_+ = \frac{1}{\kappa} \ln\left(y/k_s\right) + B = \frac{1}{\kappa} \ln\left(y e^{\kappa B}/k_s\right) \qquad \textbf{(75)}$$

with, in this case, k_s = the particle size, B = 8.5 and thus $e^{\kappa B}$ = 30. In a general way y_0 can be defined as (e.g. Booij, 1992, pp.62-65):

$$y_0 = a_1 \frac{\nu}{E|u_*|} + a_2 \frac{k_s}{30} \qquad \textbf{(76)}$$

The coefficients a_1 and a_2 allow to select the smooth wall roughness (a_1 = 1, a_2 = 0) or the hydraulic rough (a_1 = 0, a_2 = 1) empirical roughness relationships or a combination for the transition zone.

3.8.3. A continuous Law-of-the-Wall

In this section an alternative law-of-the-wall is proposed which covers the viscous sublayer and the log-region. The construction of an analytical continuous law-of-the-wall of the form $u_+(y_+)$ requires that the following conditions must be fulfilled. In the fully developed turbulent region the log-law must be reached. At the wall the following conditions hold: $u_+(0)$ = 0, $u_+'(0)$ = 1 and $u_+''(0)$ = 0 (where a prime represents a derivation with regard to y_+).

The following velocity profile can be proposed:

$$u_+ = \left(1 - e^{-y_+/y_1}\right)\left(y_1 + A \ln(1 + y_+/y_2)\right) = \frac{\left(1 - e^{-y_+/y_1}\right)}{\kappa} \ln\left(\frac{2/\kappa + y_+}{y_0}\right) \qquad \textbf{(77)}$$

with: A = 1/κ (the inverse von Karman coefficient), y_2 = 2A and:

$$y_1 = \frac{1}{\kappa} \ln(2/\kappa y_0) \qquad \textbf{(78)}$$

The full construction and the determination of the constants is presented in Appendix 1. It is

found to well represent the measurements (figure 9)[2]. For smooth walls one has $\ln(y_0^{-1})/\kappa = 5.5$ from Nikuradse's log-law, which gives $y_1 = 9.5236$. It can be seen in figure 9 that around this value the transition region starts. Therefore, the parameter y_1 is a measure of the thickness of the viscous sublayer and has a clear physical meaning. The first function describes the viscous sublayer. The second function corresponds to the log-law (and is similar to the form proposed by Christensen, 1972)[3]. In figure7 the new continuous wall law (full line) is shown together with the traditional wall law (dashed lines). The centred lines present the viscous and turbulent functions of the new law, obtained by putting $y_+ = 0$ in the other function. Notice that y_1 also equals the asymptotic value $\lim u_+(y_{+0}\to 0)$ of the turbulent profile.

The corresponding velocity gradient is given by:

$$\frac{\mathrm{d}u_+}{\mathrm{d}y_+} = e^{-y_+/y_1}\left(1+\frac{A}{y_1}\ln(1+y_+/2A)\right) + A\,\frac{1-e^{-y_+/y_1}}{y_+ + 2A} \qquad \textbf{(79)}$$

Compared to data and the (modified) Van Driest formula, the gradient does not yield such a good
agreement.

3.9. CONCLUSIONS

Provided that the velocity distribution and the shear velocity (or the corresponding head loss or pressure gradient) one can derive the velocity gradient (or viscous stress) by differentiation, the Reynolds stress distribution with eq.(45), the eddy viscosity distribution with eq.(46) or (55), the Prandtle mixing length distribution with eq.(48), and the TKE production distribution with eq.(61). However, in practice this may be invalid because no real open-channel flow is purely one-dimensional: secondary currents, generated by wall friction (no channel is infinitely wide), distort the previously presented ideal picture.

---

[2] In the transition region better agreement with data is obtained for $y_1 = 7.5$ and $y_2 = 2.2$, but then the velocity gradient near the wall deviates (becomes > 1) and the curvature at the wall is not zero.

[3] Christensen (1972) calculates the velocity profile from integration of the stress balance:
$\tau_w/\rho = u_*^2 = (\kappa u_* y + \nu)\,\partial u/\partial y$.

4. LOW-REYNOLDS EFFECTS

The traditional treatment of the wall boundary in the standard k-ε turbulence model generally does not yield correct results in the case of separation, recirculation and some other complex flow phenomena, which are related to the important influence of the fluid viscosity (Patel *et al.*, 1985). As these effects occur increasingly with reducing turbulent Reynolds numbers, one speaks of "low-Reynolds" modifications.[4]

Recent experimental data and DNS results indicate that Reynolds-number effects are also present in the inner layer (So *et al.*, 1996). See also (Yang & Shih, 1993), (Rhee & Sung, 1996) and (Hwang & Lin, 1998)

4.1. DAMPING FUNCTIONS: INTRODUCTION

The near-wall damping effects can be taken into account in the k-ε model by multiplication of the constant c_μ, c_1 and c_2 with correction factors f_μ, f_1 and f_2 respectively, which are positive functions such that $0 < f_\mu < 1$, $1 < f_1$ and $0 < f_2 < 1$ (Hanjalic & Launder, 1976). In the traditional approach (Hanjalic & Launder, 1976) they depend on two local Reynolds numbers, i.e. the turbulent Reynolds number R_t, eq.(15), and the wall Reynolds number R_y, defined as:

$$R_y = \sqrt{k}\,\frac{y}{\nu} \tag{80}$$

Abe *et al.* (1992) define another wall Reynolds number based on the Kolmogorov length or velocity scales (eqs.12 & 11):

$$y^* = \frac{y}{\eta} = \frac{u_\varepsilon y}{\nu} \tag{81}$$

Several (semi-)empirical damping functions have been proposed by various authors. An intercomparison of some of the most important low-R_t models is given by Patel *et al.* (1985).

The most popular low-Reynolds formulation is the one of Lam & Bremhorst (1981). This model has been shown to be one of the best performing (Patel *et al.*, 1985). This formulation can be implemented easily in any code. More complex forms are difficult to implement into finite element formulations (Mohammadi & Pironneau, 1993).

It should be emphasized that the majority of the damping functions proposed in the literature have been developed and calibrated for near-wall boundary layers along smooth walls and are a function of the distance from the wall. For laminarisation effects away from the wall, as around a lutocline, most of these formulations are unsuitable.

4.2. THE DAMPING FUNCTION f_μ

The damping function f_μ is introduced to modify the value of c_μ. In principle, provided

[4] The term "low-Reynolds" may cause confusion, as these laminarisation effects can also occur in flows where the global Reynolds number, based on a physical length scale, such as the water depth in open-channel flow, can be very high.

that the distributions of velocity, k and ε are known, it can be calculated from the definition of the relative eddy viscosity (Patel *et al.*, 1985):

$$f_\mu = \frac{\nu_t^+}{c_\mu \dfrac{k_+^2}{\varepsilon_+}} = \frac{\nu_t^+}{c_\mu R_t^+} = \frac{-\overline{u'v'}}{c_\mu \dfrac{k_+^2}{\varepsilon_+}\dfrac{\partial u_+}{\partial y_+}} \qquad \textbf{(82)}$$

The near-wall profile, obtained with the average experimental data from Patel *et al.* (1985) is shown in figure 10. In the case of fully-developed turbulent open-channel flow one can write:

$$f_\mu = \frac{1 - \eta - \dfrac{\mathrm{d}u_+}{\mathrm{d}y_+}}{c_\mu R_t \dfrac{\mathrm{d}u_+}{\mathrm{d}y_+}} \qquad \textbf{(83)}$$

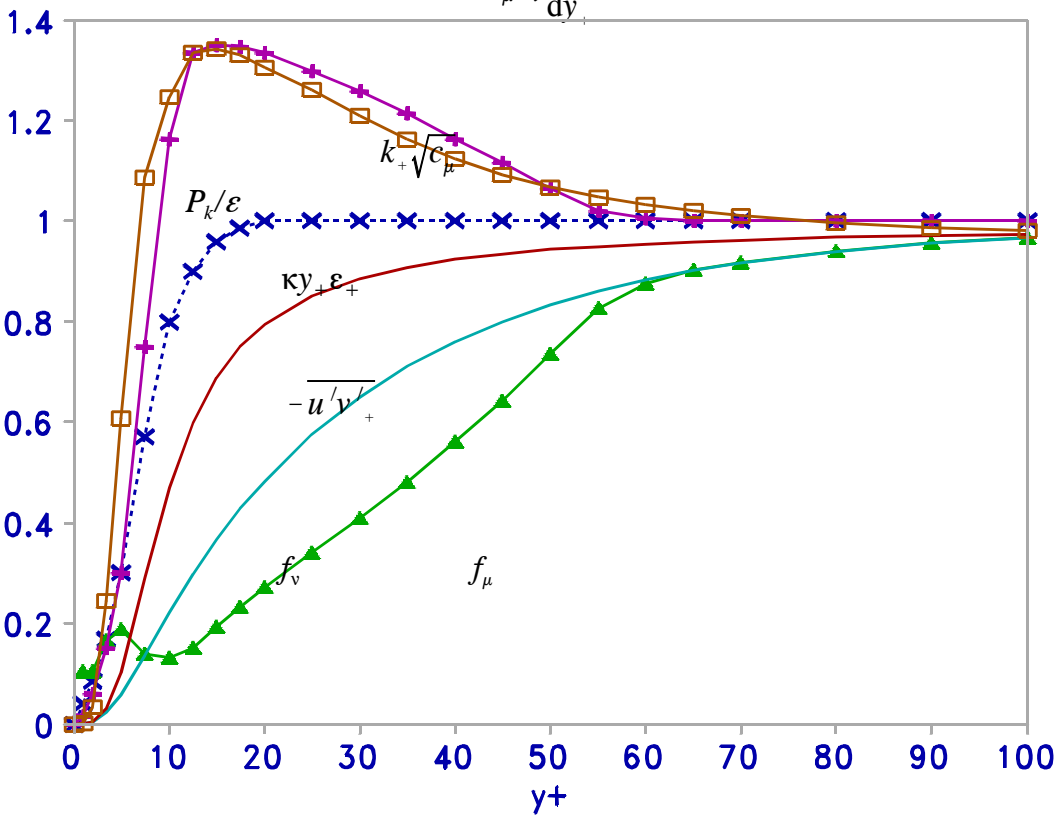

Figure 10: Profiles of the damping function f_μ and various non-dimensionalized parameters in the near-wall turbulent boundary layer.

Many empirical closure relationships have been proposed in the literature, from simple ones to very complex ones. Patel *et al.* (1985) mention three criteria which can be employed to evaluate these formulations: (1) comparison with a distribution constructed from experimental or DNS data; (2) their influence on the logarithmic region, where f_μ should reach the asymptotic value 1; (3) the implied near-wall distribution of the Reynolds stress.

The first damping functions proposed were only a function of R_t (e.g. Launder & Sharma, 1974). Most low-*Re* formulations are developed for wall boundary layers are expressed in terms of wall distance and R_t. Several of them are listed in the review by Patel *et al.* (1985). The distribution near the wall of eddy viscosity is generally obtained by introducing the Van Driest damping function (Patel *et al.*, 1985). A typical form is given by:

$$f_\mu = \left(1 - \mathrm{e}^{-(R_y/A)^{3-m}}\right)^m \left(1 + \frac{B}{R_t^{\,n}}\right) \qquad \textbf{(84)}$$

When $m = 2$, the first factor actually represents the square of the mixing length damping factor, corresponding to eq.(50). Nagano & Hishida (1987) even propose to simply use the square of the Van Driest damping function. Some values for the parameters proposed in the literature are given in the following table.

Reference	A	m	B	n
Lam & Bremhorst (1981)	60	2	20.5	1
Nagano & Hishida (1987)	26.5	2	0	0
Abe et al. (1992)	14	2	$5\ \exp(-(R_t/200)^2)$	3/4
Park & Sung (1995)	80	1	$10\ \exp(-(R_y/A)^2)$	1.25

According to Nagano & Tagawa (1990) the damping function should satisfy the limiting behaviour for $y \to 0$: $f_{\mu 1} \div y^{-1}$, which is guaranteed by their formulation. This is confirmed by DNS data (Hwang & Lin, 1998).

Lam & Bremhorst (1981) argue that in the near-wall layer part of the damping is directly attributed to the presence of the wall itself (i.e. the non-slip condition) and propose to write f_μ as the product of two functions, the first function of R_t, as before, and the second as a function of the wall Reynolds number R_y, defined by eq.(80). The Lam-Bremhorst damping function reads:

$$f_\mu = \left(1 - \exp(-0.0165 R_y)\right)^2 \left(1 + \frac{20.5}{R_t}\right) \qquad \textbf{(85)}$$

Park & Sung (1995) propose a more complex formulation. They define $f_\mu = f_{\mu 1} f_{\mu 2}$, with $f_{\mu 1}$ the wall function:

$$f_{\mu 1} = \left(1 - e^{-(R_y/80)^2}\right)\left(1 + 10\,\frac{e^{-(R_y/80)^2}}{R_t^{\,5/4}}\right) \qquad \textbf{(86)}$$

$f_{\mu 2}$ accounts for the non-equilibrium effect. From experimental findings it is known that c_μ varies as a function of P_k/ε (Rodi, 1972), also away from the wall where the wall-induced damping factor $f_{\mu 1} = 1$. In the non-equilibrium region ($P_k/\varepsilon \neq 1$) a relationship has been derived from an algebraic stress model for an attached 2D flow by Rodi (1972), which is written with redefined constants as (Park & Sun, 1995):

$$f_{\mu 2} = C_{\mu 1} \frac{C_{\mu 2} + C_{\mu 3} P_k/\varepsilon}{(C_{\mu 2} + P_k/\varepsilon)^2} \qquad \textbf{(87)}$$

with constant values: $C_{\mu 1} = 2.62$, $C_{\mu 1} = 1.2$, $C_{\mu 3} = 0.646$, obtained from fitting with Rodi's experimental data. One could question whether some effects are not accounted for twice.

The near-wall distribution of the Reynolds stress should be proportional to y^3 (see Section 3.2). This implies that at the wall $f_\mu \sim y^{-1}$ (e.g. Nagano & Tagawa, 1990), resulting in an infinite value at the wall. This condition is not fulfilled by the Lam-Bremhorst function ($f_\mu \sim y^0$), neither by any of the other functions discussed by Patel *et al.* (1985). DNS data (Hwang & Lin, 1998) indeed show that f_μ decreases near the wall. The near-wall asymptotic behaviour implies that f_μ tends to infinity at the wall. This may cause numerical problems if the first grid point is chosen too close to the wall.

Based on DNS data the author has attempted to redefine f_μ not as a product, but as a superposition of two functions:

$$f_\mu = A \exp(-y_+/B) + f(R_t) \qquad \textbf{(88)}$$

with: $A = 0.3$ and $B = 2$, based on figure 4 in (Hwang & Lin, 1998). But this does not fulfil the near-wall asymptotic behaviour either, unless the negative exponential is replaced by $1/y_+$ and the coefficient recalibrated accordingly.

When the realisable time scale is taken into account, one should look at the near-wall asymptotic behaviour of $f_\mu' = f_\mu/f_T$, which is $f_\mu' \sim y$. The previous equation can then be redefined as:

$$f_\mu = f_T \left(A\, y \exp(-y_+/B) + f(R_t) \right) \qquad \textbf{(89)}$$

This formulation fulfills the theoretical conditions at the wall, provided that the near-wall asymptotic behaviour of $f(R_t)$ should be proportional with y^2, i.e. $R_t^{1/2}$. e.g.:

$$f(R_t) = 1 - \exp\left(-\sqrt{R_t}/C\right) \qquad \textbf{(90)}$$

Remark: Interestingly, the analysis of the numerically generated data using a modified Lam-Bremhorst low-*Rt* model (where "modified" implies using LB in the form of eq.89) by the author strongly suggests that in the near-wall layer ($y_+ < 3$), the following equality seems to hold:

$$\frac{P_k}{\varepsilon} = \frac{c_\mu R_t}{\kappa y_+} \qquad (y_+ < 3) \qquad \textbf{(91)}$$

This would imply that the eddy viscosity damping function in the viscous sublayer can be described by:

$$f_\mu = \frac{\varepsilon_+}{\kappa y_+} \qquad (y_+ < 3) \qquad \textbf{(92)}$$

and the eddy viscosity itself as:

$$\nu_t^+ = \frac{c_\mu k_+^2}{\kappa y_+} \qquad (y_+ < 3) \tag{93}$$

The damping function fulfils the theoretical near-wall asymptotic behaviour. By lack of theoretical proof, this may be pure coincidence.

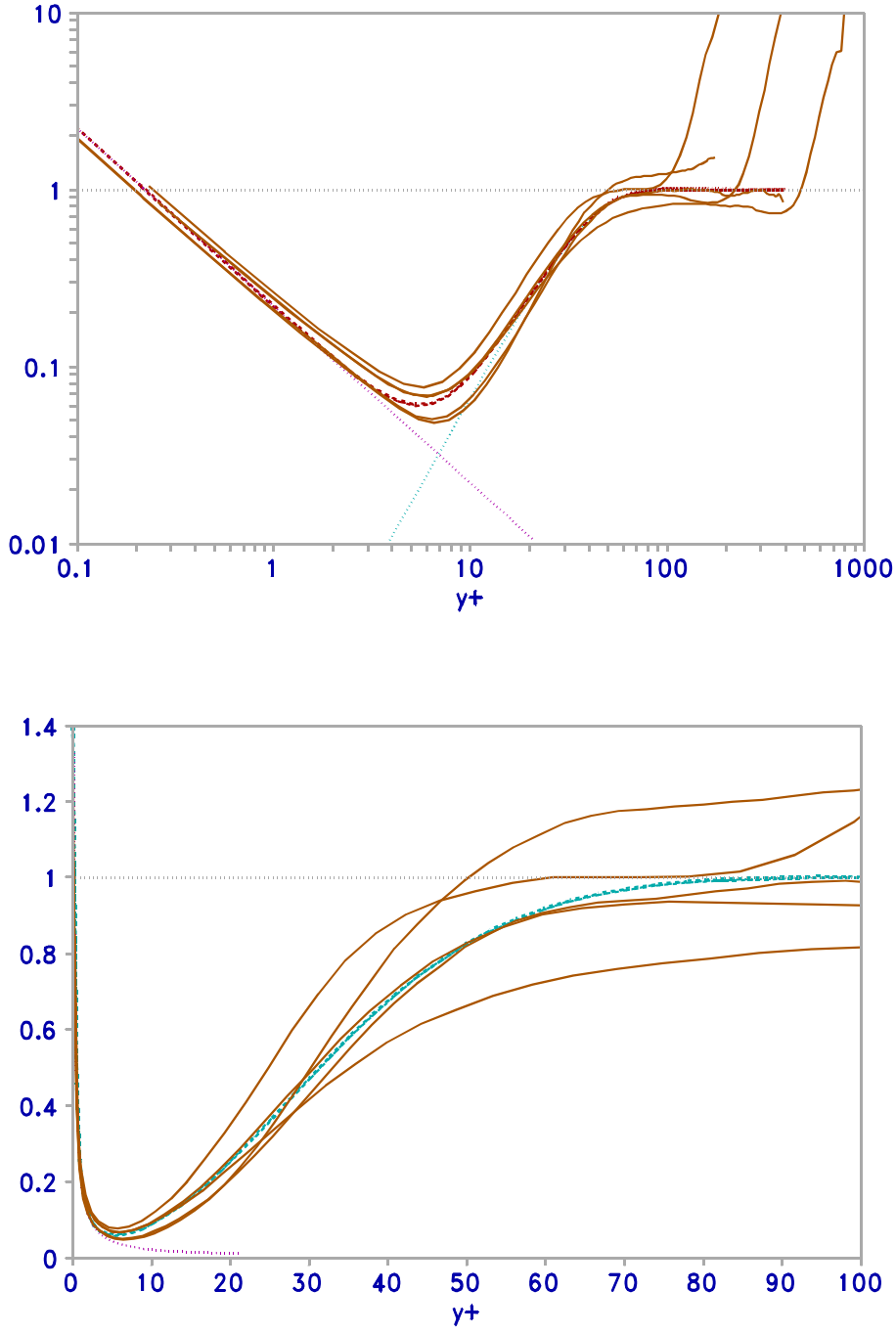

Figure 11: The damping function f_μ as a function of wall distance for various DNS data (Kim *et al.*, 1987; Kim, 1989; Spalart, 1988). Dotted lines = approximated variation in the near wall and transition regions. Dashed line = approximated with eq.(94) and $B = 38$.

The best approximation for the damping function, expressed as a function of the wall distance, is:

$$f_\mu = \frac{A}{y_+} + 1 - \exp(-By_+^2) \qquad \textbf{(94)}$$

It was found that $A = 0.2$, while B seems to be case dependent (figure 11).

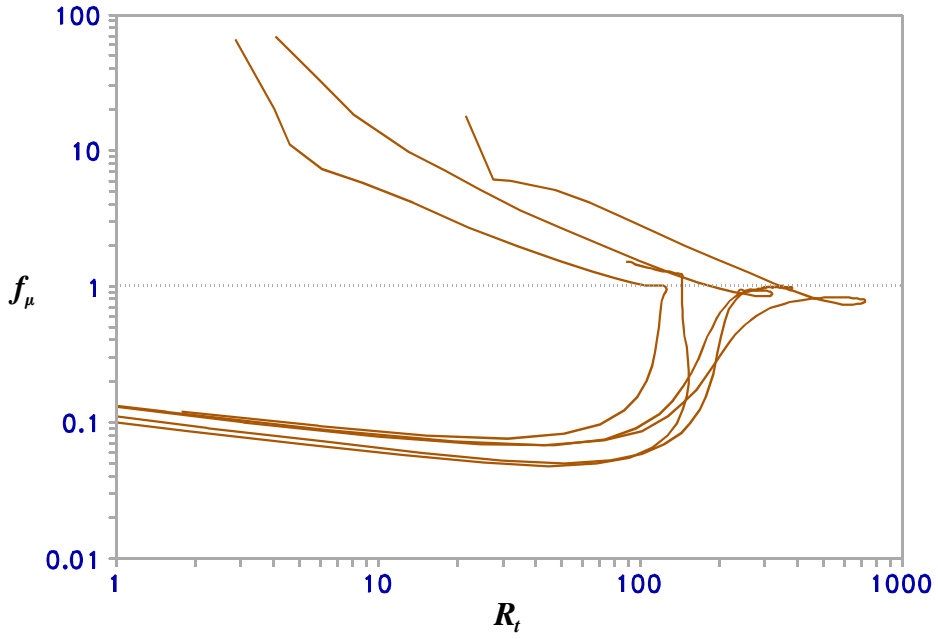

Figure 12: The damping function f_μ as a function of turbulent Reynolds number for various DNS data (Kim *et al.*, 1987; Kim, 1989; Spalart, 1988).

Figure 12 shows the variation of the damping function as a function of the turbulent Reynolds number R_t. It is clear that there is no unique relationship. The values greater than 1 are reached where the boundary layer transits to the uniform, laminar main flow outside the boundary layer. Also the channel flow case with small dimension shows an increase of f_μ near the centerline, while the other case gives a nearly unique relationship. The DNS data seem to suggest that the resolutions were not fine enough.

When using the Van Driest mixing length (eq.51) and the relationship between ν_t^+ and ℓ_+ (eq.55), the second equality of eq.(82) gives an "exact" formulation in function of y_+ and R_t^+. It is surprising that nobody mentions this solution.

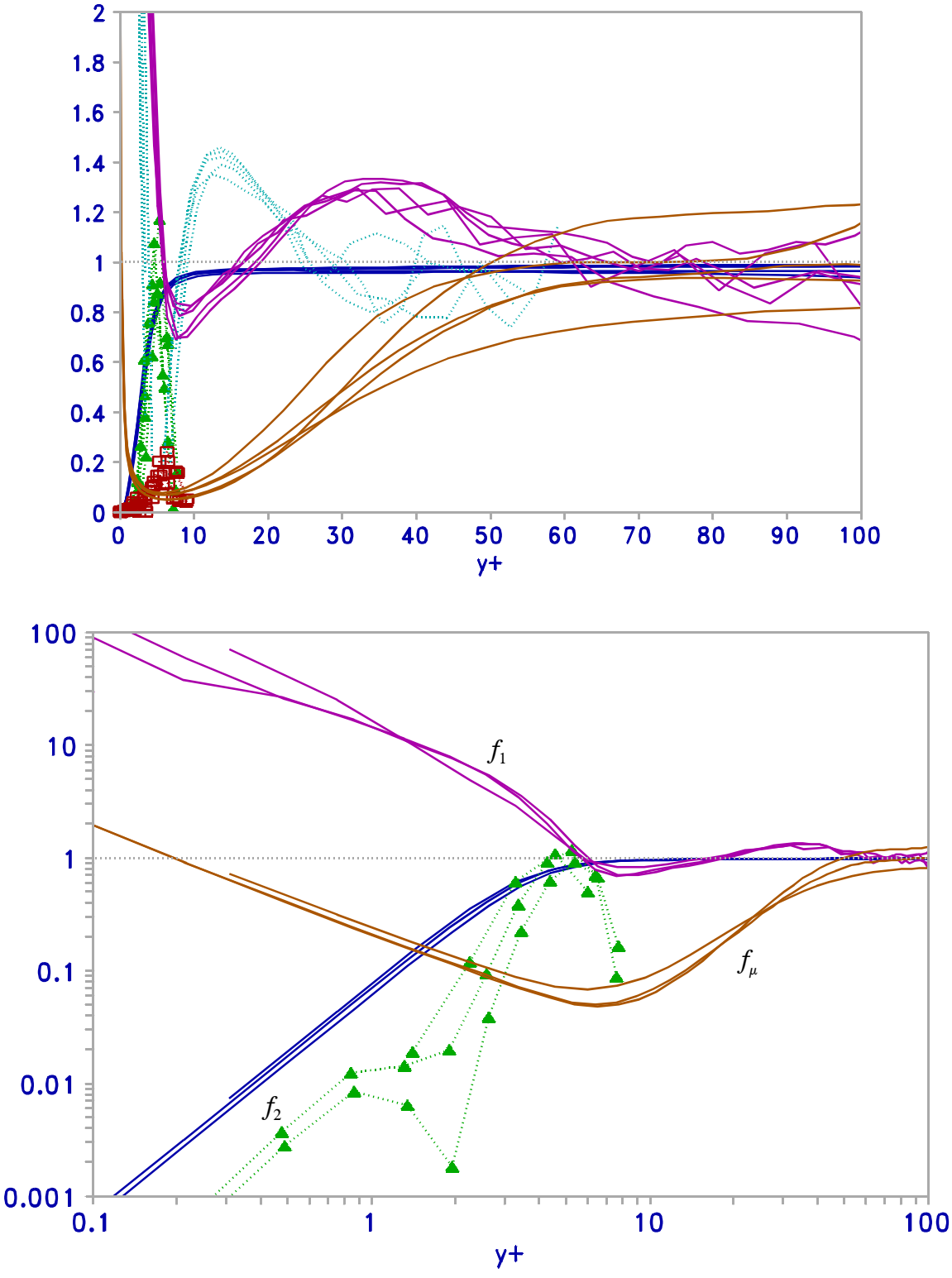

Figure 13: Damping functions derived from DNS data.
▲ = estimation of f_2 with eq.(95).
(Top figure: dotted lines = f_1 and □ = f_2 estimated using k balance to compute ε)

4.3. THE DAMPING FUNCTION f_2

"The function f_2 is introduced primarily to incorporate low-R_t effects in the destruction term of the ε-equation. The physical basis for this is provided by experiments in the final period of the decay of isotropic turbulence, which show that the exponent n in the decay law $k \sim x^{-n}$ changes from 5/4 at high Re to 5/2 in the final stage." (Patel *et al.*, 1985).

The ε-equation at the wall reduces to:

$$\nu \frac{\partial^2 \varepsilon}{\partial y^2} = f_2 c_2 \frac{\varepsilon^2}{k} \qquad \textbf{(95)}$$

A truncated series expansion of ε near the wall is:

$$\varepsilon = \varepsilon_0 + by^2 + cy^3 \qquad (y_+ \ll 1) \qquad \textbf{(96)}$$

Hence, in order to obtain the ε-equation consistent at the wall, it is required that $f_2 \sim y^2$ near the wall (Patel *et al.*, 1985).

Most of the functions used are of the form:

$$f_2 = 1 - A \exp\left(-(R_t/B)^2\right) \qquad \textbf{(97)}$$

Several models employ the parameter values $A = 0.3$ and $B = 1$, proposed by Launder & Sharma (1974). The values $A = 0.22$ and $B = 6$, used by Chien (1982), based on the work of Hanjalic & Launder (1976), yields the best fit for the grid-turbulence experimental data of Batchelor & Townsend (1948). In the popular Lam-Bremhorst (1981) model the parameter values are $A = B = 1$. The choice $A = 1$ is justified by the fact that ε and its first and second derivative should have finite values at the wall.

Park & Sung (1995) define a more complex function f_2 by multiplying the above form with a factor for the wall proximity, which were obtained by fitting DNS data from Mansour *et al.* (1988).

When the realisable time scale is introduced, the damping function f_2 should be modified accordingly: $f_2 = f_2'/f_T$. Because the asymptotic behaviour of $1/f_T$ is $R_t^{1/2} \sim y^2$, the asymptotic behaviour of f_2' should be a constant value (probably 1). Analysis of DNS data, by applying eq.(95) to the data results in data points which lie approximately along the realisable time scale factor (see fig.13), suggesting that the choice $f_2 = 1/f_T$ seems very acceptable. Numerical simulations show that the choice $f_2 = 1/f_T$ yields less dissipation at the wall compared to the Lam-Bremhorst function.

4.4. THE DAMPING FUNCTION f_1

The background for the introduction of the function f_1 for the production terms in the ε-equation is related to the observed underestimation of the near-wall dissipation (or diffusion) obtained with the standard equation. This has become particularly clear with DNS simulations which show that the maximum of ε is reached at the wall itself (e.g. Spalart, 1988; Hwang & Lin, 1998). Several ways of modification have been proposed.

Launder & Sharma (1974) proposed to add so called pressure diffusion terms in the k and the ε equation. This idea has been followed by Chien (1982) and Hwang & Lin (1982) among others.

Another way to increase the near-wall diffusion is to define correction factors for the

model parameters σ_k and σ_ε (e.g. Nagano & Shimada, 1990; Park & Sung, 1995). Hwang & Lin (1998) have combined the two methods and succeed to simulate the maximum of ε at the wall.

The third method is the introduction of the damping function f_1, as proposed by Lam & Bremhorst (1981). They proposed the function:

$$f_1 = 1 + (0.05/f_\mu)^3$$

without much justification. Park & Sung (1995), in addition to modifying σ_k and σ_ε, define f_1 as a function of the production-dissipation balance:

$$f_1 = A + (1 - A)\frac{P_k}{\varepsilon} \qquad \textbf{(99)}$$

with $A = 0.95$.

When the realisable time scale is introduced, the damping function f_1 should be modified accordingly: $f_1 = f_1'/f_T$. With the assumption of $f_2 = 1/f_T$, the function f_1 can be calculated for DNS data from the ε-equation:

$$\frac{\mathrm{d}}{\mathrm{d}y_+}\left(\left(1 + \nu_t^+/\sigma_\varepsilon\right)\frac{\mathrm{d}\varepsilon_+}{\mathrm{d}y_+}\right) + \frac{f_1 c_1 \nu_t^+}{T_t^+}\frac{\mathrm{d}u_+^{\,2}}{\mathrm{d}y_+} = \frac{f_2 c_2 \varepsilon_+}{T_t^+} \qquad \textbf{(100)}$$

The resulting profile is shown in figure 13. The shape suggests a close relationship to f_μ. The ratio f_1/f_μ can be approximated by the simple analytical function:

$$\frac{f_1}{f_\mu} \cong \frac{A + (y_+/B)^n}{1 + (y_+/B)^n} \qquad \textbf{(101)}$$

with parameter values $A = 100$, $B = 2$ and $n = 3/2$. Using the analytical approximation for f_μ, one obtains a reasonable fit for f_1 of the DNS data (see fig.13).

4.5. THE COEFFICIENT σ_k

When the same procedure is applied to the dissipation rate, calculated from the k-equation, using the DNS data for k, another profile of ε is obtained, which shows again the local minimum near the wall. Notice that the asymptotic behaviour near the wall and in the fully developed turbulent region are approximately the same. The corresponding damping function f_1 has another shape now and becomes negative where ε reaches its local minimum. This does not seem correct, as this would imply that there should be negative production. This can only be resolved by increasing the diffusion of k, i.e. by making the parameter σ_k variable. The variation of σ_k can be reconstructed from the DNS data using the k-equation:

$$\sigma_k = \frac{\nu_t^+ \dfrac{\mathrm{d}k_+}{\mathrm{d}y_+}}{\displaystyle\int_0^{y_+}\left(\varepsilon_+ - P_k^+\right)\mathrm{d}y_+ - \frac{\mathrm{d}k_+}{\mathrm{d}y_+}} \qquad \textbf{(102)}$$

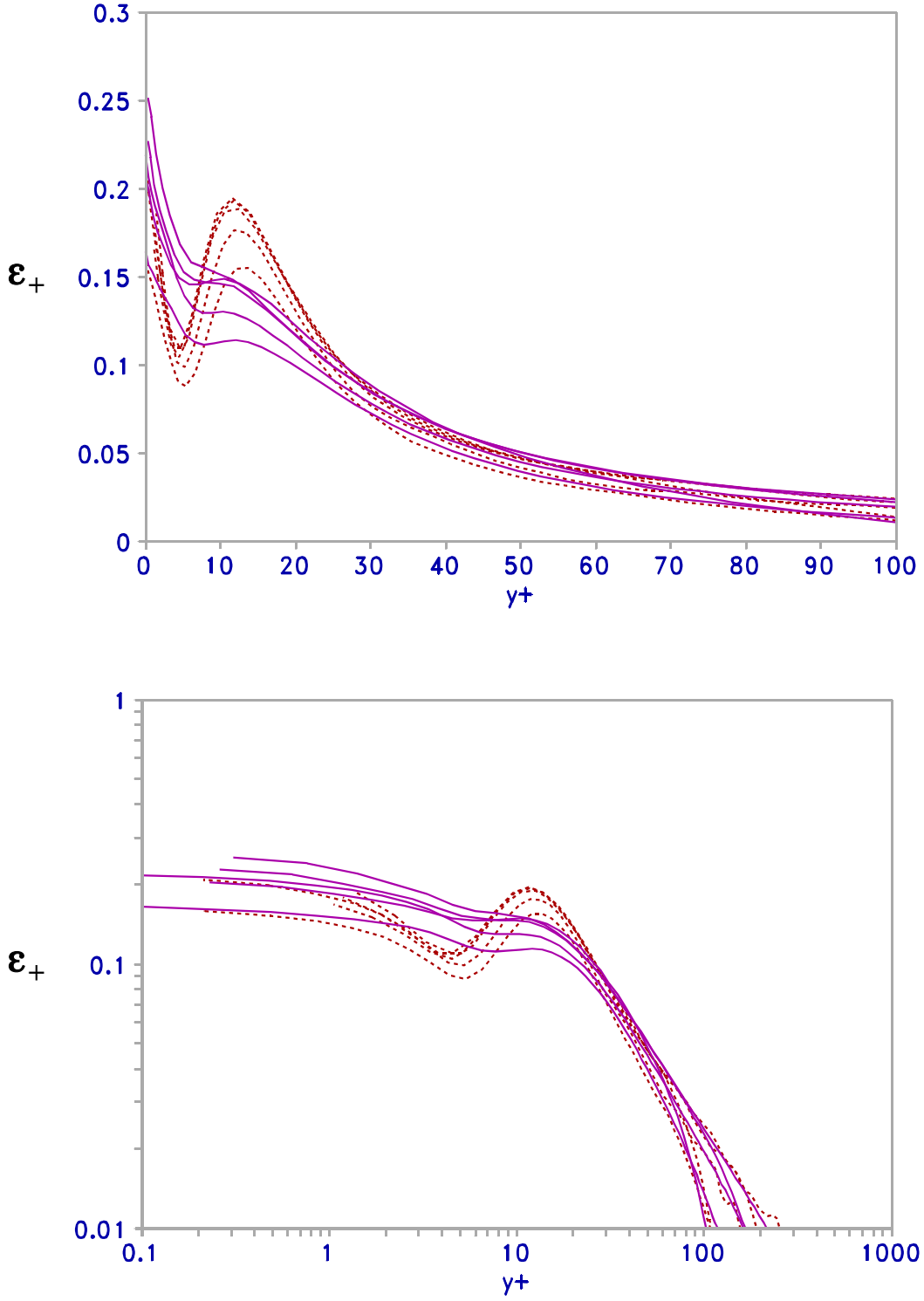

Figure 14: Near-wall distribution of the non-dimensional turbulent dissipation rate ε_+. Full line = DNS data; dashed line is reconstructed with the *k*-equation, assuming $\sigma_k = 1$.

The resulting profiles in the near-wall region are shown in figure 14. It shows that σ_k tends to infinity at $y_+ \approx 11$ and changes sign.

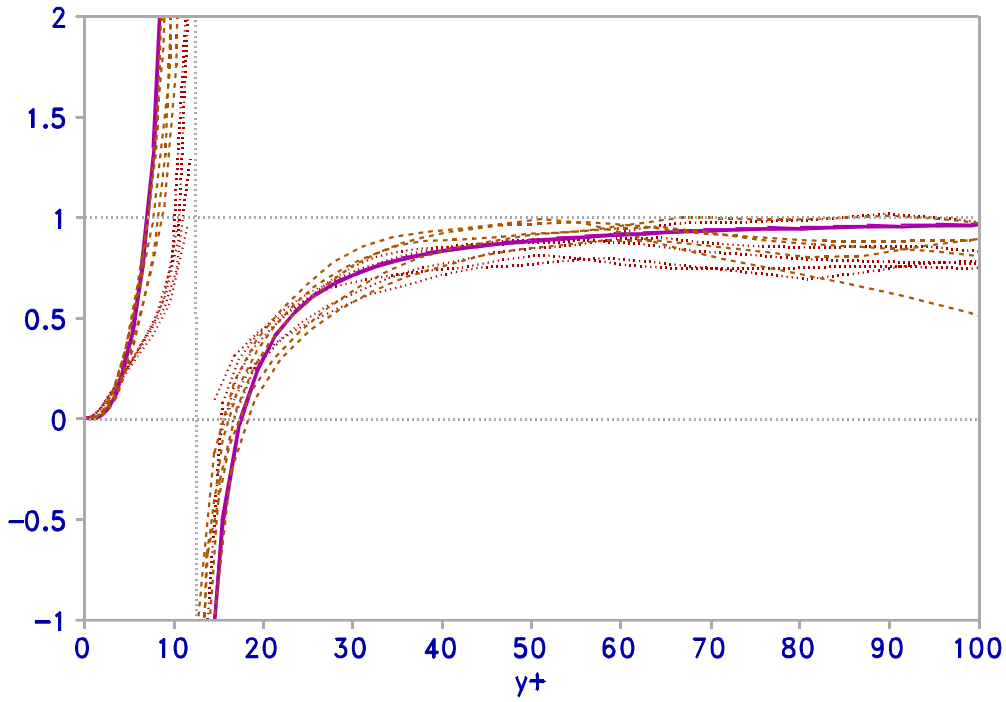

Figure 15: Near-wall distribution of σ_k. Dashed lines = reconstructed from DNS data with eq.(101); dotted lines = reconstructed from DNS dissipation data; full line = proposed fit (eq.102).

A surprisingly good fit for σ_k is found with (fig.15):

$$\sigma_k = \frac{1}{f_T}\left(sign(y_+ - Y_0) - \frac{1}{(y_+/Y_0)^{3/2} - 1} \right) \qquad \textbf{(103)}$$

For practical implementation into a numerical code, one should work with the inverse of σ_k around the singular point, i.e. in the range where $|\sigma_k^{-1}| > 1$.

The location of the singular point corresponds to the distance from the wall where the turbulent diffusion reaches its minimum and k its maximum, which lies slightly further from the wall ($y_+ \cong 15$) then the location of the maximum of production (see fig. 8). The difficult aspect is the occurrence of a layer where the turbulent diffusion becomes negative and where the total diffusion coefficient has a singular point. This actually reflects one of the short-comings of the k-ε equations, which assumes isotropic turbulence. Isotropy so close to the wall is physically impossible, as fluctuations in the direction of the wall are hindered by its presence.

4.6. AN APPROACH FOR THE CONSTRUCTION OF (NEAR-WALL) DAMPING FUNCTIONS

Near-wall damping functions actually are defined as the behaviour in the near-wall field, relative to that in the far field. The asymptotic behaviour for large y_+ corresponds to fully developed turbulent flow where the log-law is valid. One finds following corresponding distributions.

- Velocity: log-law
- Velocity gradient: $\partial u_+/\partial y_+ = 1/\kappa y_+$
- Reynolds stress: $-\overline{uv}_+ = 1 - \dfrac{1}{\kappa y_+}$
- Relative eddy viscosity: $\nu_t/\nu = \kappa y_+$.
- Kinetic energy: $k_+ = c_\mu^{-1/2}\ (= 10/3)$
- Dissipation rate: $\varepsilon_+ = 1/\kappa y_+$

The data of figures 2-4 show that the log-law and the assumption of equilibrium ($P_k/\varepsilon = 1$) is only approximately valid for distances from the wall of $y_+ > 60$ (and far enough from other boundaries where diffusive effects become important, such as a free surface).

A general and systematic way to compute the damping functions is to define damping functions for each basic parameter as the ratio of the actual value to the asymptotic log-region value.

- Velocity:

$$f_u = \frac{\kappa u^+}{\ln\left(1 + y^+/y_0^+\right)} \qquad \textbf{(105)}$$

Note that a modified log-law is used to ensure positive results up to the wall.

- Velocity gradient or viscous stress:

$$f_{u'} = \kappa y^+ \frac{\mathrm{d}u^+}{\mathrm{d}y^+} \qquad \textbf{(106)}$$

- Reynolds stress:

$$f_\tau = \frac{-\overline{u'v'}^+}{1 - 1/\kappa y^+} \qquad \textbf{(107)}$$

As this damping function yields negative values close to the wall, one could alternatively use:

$$f_\tau = -\overline{u'v'}_+ = \frac{-\overline{u'v'}}{\rho u_*^2} \qquad \textbf{(108)}$$

- Mixing length:

$$f_\ell = \frac{\ell_+}{\kappa y_+} \tag{109}$$

- Eddy viscosity damping factor:

$$f_\nu = \frac{\nu_t^+}{\kappa y_+} \tag{110}$$

- TKE damping factor:

$$f_k = k_+ \sqrt{c_\mu} \tag{111}$$

- Dissipation rate damping factor:

$$f_\varepsilon = \kappa y_+ \varepsilon_+ \tag{112}$$

- Production damping factor:

$$f_P = \kappa y_+ P_k^+ \tag{113}$$

Several of these are shown in figures 10 and 16. In a next step, these basic damping functions can be combined to yield other damping functions. It is then easily found that:

$$f_\mu = \frac{f_\nu f_\varepsilon}{f_k^2} = \frac{f_\tau^2}{f_{EB} f_k^2} = \frac{f_\ell \sqrt{f_\tau}}{f_{R_t}} \tag{114}$$

where: $f_{EB} = f_P/f_\varepsilon = P_k^+/\varepsilon_+ = P_k/\varepsilon$, the energy balance damping function. Returning to the Prandtl mixing length approximation one can also write:

$$f_\mu = f_{c_D} f_\ell^2 f_{u'} \tag{115}$$

According to eq.(5) one can write:

$$f_\ell = \frac{f_{c_D} f_k^{3/2}}{f_\varepsilon} \tag{116}$$

Eliminating f_{cD} yields:

$$f_\mu = \frac{f_\ell^3 f_\varepsilon f_{u'}}{f_k^{3/2}} \tag{117}$$

Returning to the expression of the eddy viscosity as a function of the turbulent time scale (eq.27) and the definition of the realisable time scale, it becomes clear that the realisability

factor f_T and the damping function f_μ are related as:

$$f_\mu = f'_\mu f_T \tag{118}$$

with:

$$f'_\mu = \frac{f_\nu f_\varepsilon}{f_k^2 f_T} \tag{119}$$

The damping function f'_μ has a zero value at the wall.

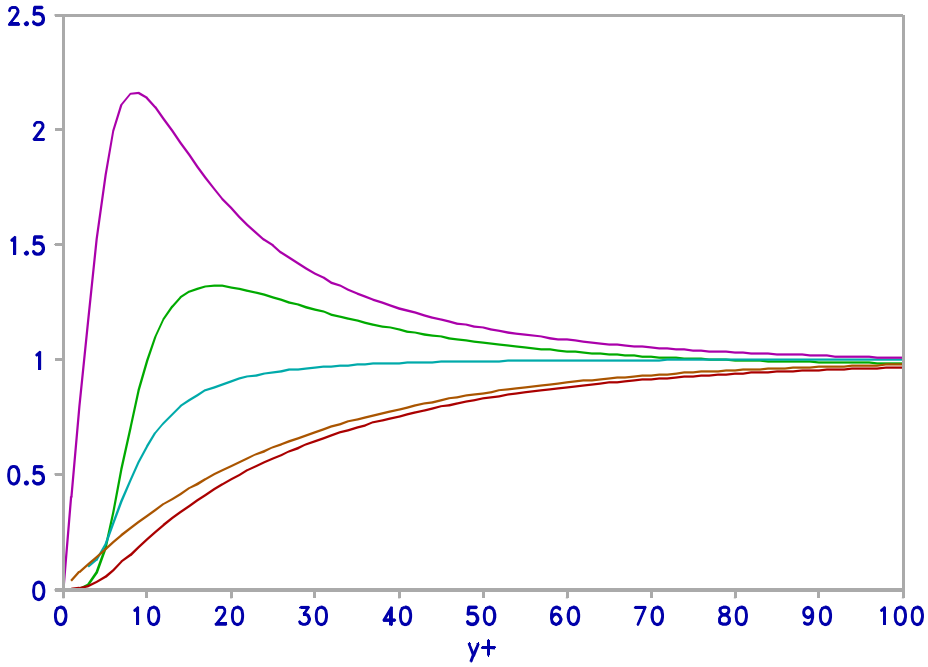

Figure 16: Curves from top to bottom: $\kappa y_+ du_+/dy_+$, $\kappa y_+ P_k^+$, $-u'v'/(1-1/\kappa y_+)$, $\ell_+/\kappa y_+$, $\nu_t^+/\kappa y_+$

Combinations of damping functions reveal several interesting features. In the sublayer ($y_+ < 20$) it is found that:

$$f_\mu = \frac{c_\mu}{f'_u \dfrac{du_+}{dy_+}} = \frac{c_\mu}{\kappa y_+ \left(\dfrac{du_+}{dy_+}\right)^2} \tag{120}$$

and:

$$f_P = c_\mu^2 R_t \tag{121}$$

In the laminar wall-layer ($y_+ < 3$) it is found that:

$$f_\mu = \frac{c_\mu}{\kappa y_+} \tag{122}$$

because the non-dimensional velocity gradient becomes 1. For the entire sublayer ($y_+ < 100$) an excellent match is found with:

$$f_\mu = \frac{c_\mu}{\kappa y_+ \dfrac{\mathrm{d}u_+}{\mathrm{d}y_+}\left(\dfrac{\mathrm{d}u_+}{\mathrm{d}y_+} + A\right)} \tag{123}$$

In order to obtain $f_\mu = 1$ in the far field, one should have $A = c_\mu$. But the DNS data yield various values of f_μ, even > 1 in the far field. Each case can be modified individually by writing $A = \alpha c_\mu$. The correction factor α reaches values in the range 0.4-1, apparently increasing when the layer thickness increases. Rodi (1972) already found that c_μ is a function of the ratio P/ε. Equation (124) does not allow a good approximation near the outer boundary of the DNS experiments used throughout this report.

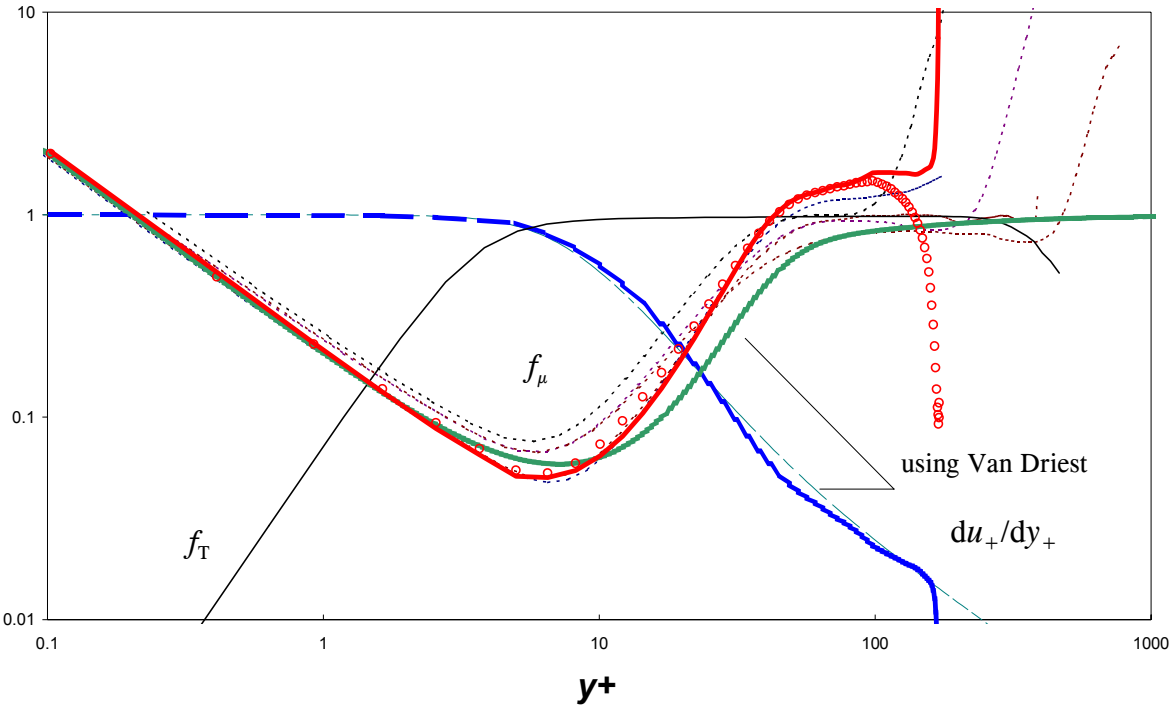

Figure 17: Comparison between eq.(124), with $\alpha = 0.41$, and DNS data (circles, open-channel flow data from Knowlton; dotted lines = the other DNS data used in this report). Lower full line = eq.(123) using Van Driest profile and $\alpha = 1$.

The damping functions f_1 cannot be reconstructed in a similar way, probably because it is suspected that the coefficient σ_ε is not constant within the wall layer. In the laminar wall-layer ($y_+ < 3$) it is found that:

$$f_1 = \frac{f_T f_k}{\kappa f_\varepsilon} \tag{124}$$

4.7. *WALL ROUGHNESS*

Previous approximations are all based on data for smooth walls. Nowhere does a roughness parameter enter the empirical correction factors. This is a severe limitation for applications in nature.

The first correction was proposed by Van Driest (1956):

$$\nu_t = (F\kappa y)^2 \frac{\partial u}{\partial y} \tag{125}$$

with:

$$F = 1 - \exp\left(-y_+/26\right) + \exp\left(-2.3\, y_+/k_s^+\right) \tag{126}$$

Krogstad (1991) proposed for large roughnesses:

$$F = 1 - \exp\left(-\frac{y_+}{26}\right) + \exp\left(-\frac{y_+}{26}\,(70/k_s^+)^{3/2}\right)\sqrt{1+\exp(-70/k_s^+)} \tag{127}$$

A new model which includes sand-roughness has been proposed by Zhang *et al.* (1996):

$$f_\mu = 1 - \exp\left(-(y_+/42)^2\right) + \exp\left(-25\, y_+/k_s^+\right)\sqrt{k_s^+/200} \tag{128}$$

and:

$$f_1 = 1 + \exp\left(\frac{-k_s^+}{1+0.1\,k_s^+}\right)\left(\frac{9.2}{1+y_+}\right)^6 \tag{129}$$

The latter formulations have successfully been implemented by Rocabado (1999).

4.8. DRAG REDUCTION

Deviations from the traditional law of the wall have been reported under a wide variety of conditions, yielding reduced friction losses under similar energetic conditions. This phenomenon has become known as “drag reduction”. Reduced friction losses in turbulent suspension flow were first reported by Toms (1949) for a polymer suspension. It occurs under conditions like:

- moving or vibrating walls
- specific wall surfaces

- certain polymeric additives (Sellin *et al.*, 1982)
- clay suspensions (Gust, 1976).

The general characteristics are related to a reduction of the shear velocity for the same mean flow rate, or an increase of the mean flow rate for the same energy input. For instance, in the case of steady open-channel flow, the shear velocity is fixed and determined by the pressure gradient G_p ($\tau_w = H\, G_p$). When sediment is added, an increase of the velocity is observed.

Non-dimensionalized velocity profiles show an increase of the viscous sublayer and a shift of the log-law to higher values of u_+. An increase of u_+ is not surprising when the shear velocity decreases. This can easily be confirmed theoretically, especially if the same roughness reference is maintained. From the viscous law one finds:

$$u_* = \sqrt{\frac{u\nu}{y}} \tag{130}$$

Assuming a case where the velocity remains the same, the only way to reduce the shear velocity is that the thickness y should increase. A shift of the log-law corresponds to an increase of the inverse roughness parameter E or a decrease of the equivalent roughness height.

Analysis of the experiments by Gust (1976) learns:
- the von Karman coefficient is not affected (at least for the low concentrations)
- rise of log-line implies a decrease of y_0
- increase of the viscous sublayer thickness

Models for drag reduction

The earliest approach was based on modifying the constant in the Van Driest damping function. Hassid & Poreh (1975) proposed a method for the one-equation k-ℓ turbulence model, based on the damping functions of Wolfshtein (1967):

$$\begin{aligned} \nu_t &= c_\mu k^{1/2} \ell \left(1 - \exp(-A_\mu R_k)\right) \\ \varepsilon &= \frac{c_D k^{3/2}}{\ell \left(1 - \exp(-A_D R_k)\right)} \end{aligned} \tag{131}$$

with: $R_k = k^{1/2}\ell/\nu$, $c_D = 0.416$, $c_\mu = 0.22$, $A_D = 0.23$, $A_\mu = 0.016$ and $\sigma_k = 1.53$. However, this formulation of the dissipation does not satisfy simultaneously the conditions at the wall that viscous diffusion should be balanced by dissipation and that k should be proportional to y^2. This can be resolved either by setting $A_D = c_D/2$ or by adding an extra term $2\nu k/\ell^2$ to the dissipation (Hassid & Poreh, 1975). They finally propose the following form for the dissipation:

$$\varepsilon = \frac{2\nu k}{\ell^2} + \frac{c_D k^{3/2}}{\ell} \left(1 - \exp(-A_\mu R_k)\right) \tag{132}$$

This model does not succeed to predict the peak in k.

The new "continuous" law of the wall can easily be extended to simulate drag reduction effects by introduction of a parameter D:

$$\begin{aligned} u_+ &= A \left(1 - e^{-y_+/y_{+0}}\right) \left(D + \ln(Y + y_+)\right) \\ &= \left(1 - e^{-y_+/y_{+0}}\right) \left(y_{+0} + A \ln(1 + y_+/Y)\right) \end{aligned} \tag{133}$$

The parameter Y is now defined as:

$$Y = e^{y_0/A - D} \tag{134}$$

For smooth flow $D = 1$. For drag reduction $D > 1$. However, in order to obtain a better fit with the Nikuradse coefficients, one has to take as parameter values: $y_{+0} = 5.5$, $D = 1.88$ and $A = 2.5$.

Friction

The Van Driest mixing length model gives unsatisfactory results for $Re < 10^4$: the predicted constant B in the logarithmic law of the wall is too low and the friction factor is higher than given by (Hassid & Poreh, 1975):

$$\frac{1}{\sqrt{f}} = 4 \log\left(Re\sqrt{f}\right) - 0.4 \tag{135}$$

4.9. FAR-FIELD LAMINARISATION

In stratified flow with strong gradients, the turbulence can be totally damped at the lutocline, inhibiting transmission of turbulent energy to the upper layer, if the turbulence is generated by shear with the bottom. The upper layer than (re-)laminarises.

> Remark: It would be useful to define a critical value for R_t below which low-Rt modification are required (i.e. where the standard k-ε is no longer valid). E.g. a critical value of ± 100 corresponds to the case where eddy viscosity and kinematic viscosity are roughly the same, which is at a distance $y_+ = \pm 10$. For a standard wall law one could then compute the value of y below which low-R_t modifications are necessary.

The traditional low-R_t formulation has been developed for wall bounded flows and introduces a correction function which is a function of the distance from the wall. This cannot be employed for laminarisation due to a lutocline (unless a formulation would be designed where the vertical distance from the lutocline level is used as characteristic length). Recently a few wall-distance-free formulations have been proposed in the literature.

Murakami *et al.* (1996) present an extended low-Re model which can handle laminarisation away from the wall. They started from the formulation of Abe *et al.* (1992). They define a damping function for low-Re effects (f_μ), which consists of a near-wall and a laminarisation factor:

$$f_\mu = \left(1 - \exp(-y^*/14)\right)\left(1 - \exp(-R_t^{3/4}/2.4)\right)\left(1 + 1.5/R_t^{5/4}\right) \tag{136}$$

where the first factor is the near-wall damping function, the second laminarisation effects away from the wall, the third factor serves to satisfy the limiting behaviour of wall turbulence; and one for buoyancy effects (f_B):

$$f_{Bv} = 1 + 1.08 G_k/\varepsilon \tag{137}$$

It is unclear on which grounds the splitting is done. The model results are not much better than those obtained with Launder-Sharma (1974) or Abe *et al.* (1992).

Goldberg & Apsley (1997) consider the fact that in the near-wall region the proper

velocity scale is $\sqrt{\overline{v'^2}}$ and not $k^{1/2}$ (Durbin, 1991). The eddy viscosity then is:

$$\nu_t = c_\mu^* \overline{v'^2} T_t \tag{138}$$

Hence, the damping function can be expressed as:

$$f_\mu = \frac{\nu_t^{near}}{\nu_t^{far}} = \frac{c_\mu^* \overline{v'^2}}{c_\mu k} \frac{\varepsilon}{k} T_t \tag{139}$$

Based on the analysis of Patel *et al.* (1985) the limiting value of f_μ in the near-wall can be calculated as:

$$f_\mu = A_\mu \sqrt{Re_t} \tag{140}$$

Finally, Goldberg & Apsley propose:

$$f_\mu = \frac{1 - e^{-A_\mu Re_t}}{1 - e^{-\sqrt{Re_t}}} \frac{\varepsilon}{k} T_t \tag{141}$$

where T_t is the realisable time scale and $A_\mu = 0.01$. This distance free formulation may yield values < 1 away from the wall when the eddy viscosity decreases. This makes it suitable for stratification induced damping.

Using the new realisable time scale, the damping function in the viscous sublayer, following the same procedure, becomes:

$$f_\mu = f_0 \sqrt{1 + Re_t} \tag{142}$$

with as limiting value f_0. An empirical function has to be found to link the two asymptotic behaviours.

5. TWO-LAYER MODEL

One of the advantages of the low-R_t models is the direct calculation of the shear velocity from the definition, i.e. using the velocity profile:

$$u_* = \sqrt{\nu \frac{\partial U}{\partial z}} \qquad \textbf{(143)}$$

instead of the log-law (Galland, 1996).

A major disadvantage of the low-Reynolds modelling approach is that a very fine mesh is required to capture the large gradients of U, k and ε. For large-scale application, this approach is unsuitable (too costly).

An intermediate approach is to make use of an algebraic mixing length model in the wall layer, replacing the ε-equation (Chen & Patel, 1988; Rodi, 1988; Rodi, 1991; Chen & Jaw, 1998). This method allows integration up to the wall with less refinement than the low-*Re* approach and often performs better (Chen & Jaw, 1998). Only a sensitivity to an adverse pressure gradient has been observed where the low-*Re* model remains consistent (Jaw, 1991). Implementation of Rodi's model (Toorman, 1998b) shows that the model is calibrated for smooth-wall turbulence.

The alternative method can be improved by the two-layer method (Rodi, 1991) with employs the one-equation model of Norris & Reynolds (1975).

The idea is to solve the standard high-Re equations in the domain layer away from the wall and in the wall layer apply a mixing length model. The dissipation rate can then be computed as a function of ℓ and k as:

$$\varepsilon = c_D f_D k^{3/2}/\ell \qquad \textbf{(144)}$$

with: $c_D = 0.1643$, $f_D = 1 + 5.3/R$ and $R = k^{1/2}y/\nu$. This value is imposed (instead of solving the ε-equation) as Dirichlet boundary condition in the nodes in this layer. The k-equation is still solved. The eddy viscosity is computed as:

$$\nu_t = c_\mu \sqrt{k} f_\ell \kappa y \qquad \textbf{(145)}$$

with $c_\mu = 0.5478$, $\kappa = 0.41$ and $f_\ell = 1 - \exp(-R/50.5)$ (*CHAM*, 1994).

One could also take the Van Driest damping function. However, this has the disadvantage that it requires the shear velocity.

In analogy with Hughes (1978), one could subdivide the sublayer into a viscous layer ($y_+ < 5$) and an intermediate layer between $5 < y_+ < 30$.

Implementation

Within the wall layer, the values of ε are calculated with the mixing length formula in the nodes, used as Dirichlet conditions, and in the Gauss points, used in the k equation. Only at the wall ε is not computed. However, as the value of ε at the wall is given by the condition:

$$\varepsilon_w = \nu \frac{\partial^2 k}{\partial y^2} \qquad \textbf{(146)}$$

it can be easily shown that ε_w can be computed from the parabolic k-profile in the wall element as:

$$\varepsilon_w = 2\nu \frac{k_2 - 2k_1}{\Delta y} \quad \textbf{(147)}$$

where: Δy = element size, k_1 and k_2 are the values of k at the 1st and 2nd node away from the wall.

6. MODEL INTERCOMPARISON

Based on the analysis of near-wall profiles and direct numerical simulation (DNS) data, the proposed formulations for the damping function f_μ has been extended with an additional term:

$$f_\mu = f_{\mu,0} + 0.3\exp(-y_+/2) \qquad \textbf{(148)}$$

This has the additional advantage of improving numerical stability. A new formulation for the damping function f_1 has been formulated, based on a sensitivity analysis, which does not cause the numerical problems associated with the one proposed by Lam & Bremhorst (1981).

Previous preliminary results (Toorman, 1997; Toorman, 1998a) have been obtained with inclusion of the wall-layer into the computational domain without properly correcting for the viscous damping effects near the wall, resulting in wrong values of the wall stress. Presently, an intercomparison between various wall boundary treatment methods is carried out, looking at the traditional implementation of the law-of-the-wall, low-Reynolds treatment and the hybrid two-layer method of Rodi (1991). All these methods have been implemented in the code FENST. The results (fig.18) show that the high-*Re* and the 2-layer approach yield the same result and slightly underestimate the velocity in the log-region. A good simulation of the 1D velocity profile can be obtained with different damping functions (fig.18a). The results show that k is the most sensitive parameter in the near-wall layer up to a distance from the wall of $y_+ = \pm 300$. Values of ε only vary significantly in the viscous sublayer and the transient layer ($y_+ < 20$).

Future work

Problems to be looked at are:

- *Identification of the different damping effects* in order to separate wall-distance dependent effects from other (such as sediment induced) damping effects. This problem will be hard to solve by lack of the necessary experimental data.

- *Reynolds number dependence*: experimental and DNS data clearly show that the non-dimensionalized profiles of k and ε are dependent on the global Reynolds number. This implies that f_μ is not a unique function.

- *Roughness and drag reduction*: Most damping functions for near-wall turbulence, found in the literature, have been developed (i.e. tuned) for smooth walls and cannot be used for other surface roughnesses. For sand bottoms, where the bottom friction increases, roughness dependent damping functions have been developed by Zhang *et al.* (1996). For drag reduction, where velocities and the viscous sublayer thickness increase, nothing is known. However, during the calibration of the modified damping functions it was found that certain parameters in the damping functions can be related to the roughness and allow to predict both rough wall turbulence as drag reduction.

- *Mesh dependence* and mesh size requirements need further study. In particular, for large scale applications, a solution on an acceptable vertical grid size distribution need to be found which is computationally feasible.

Fig.18.a: Velocity profile: symbols = data Comte-Bellot (1965) (Re = 57000), dashed line = law-of-the-wall, full lines = various low-Re solutions obtained with FENST (LB = modified Lam-Bremhorst, 1981; MK = modified Murakami *et al.*, 1996; and a new formulation). The lowest curve is obtained with the two-layer approach (2L = Rodi, 1991) and nearly coincides with the standard high-Re solution (y_+>80).

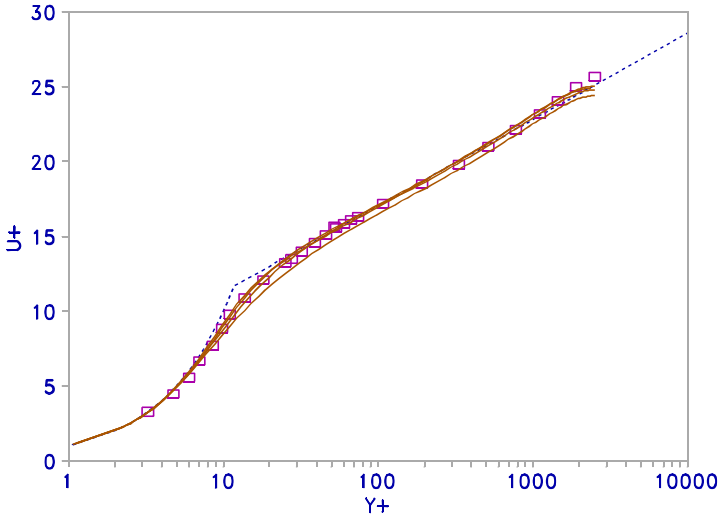

Fig.18.b: Calculated turbulent kinetic energy (k = dashed lines) and dissipation rate (ε = full lines) near the wall. Dotted line = asymptotic behaviour of $\varepsilon_+ = 1/\kappa y_+$.

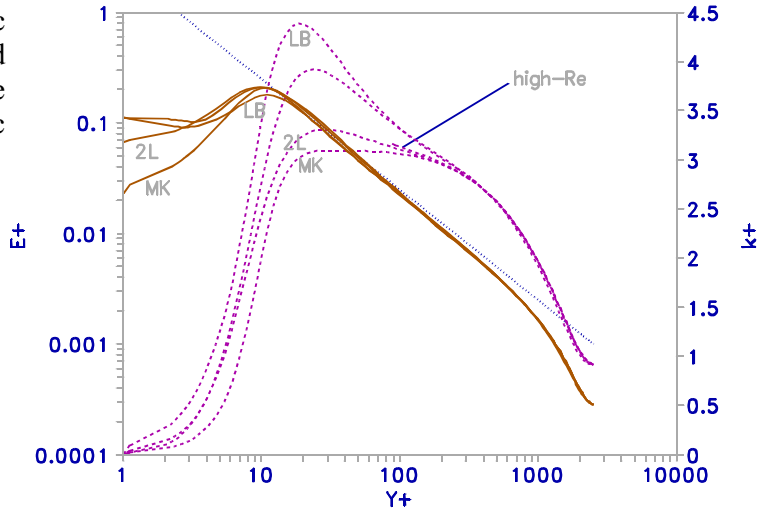

Fig.18.c: Near-wall damping for smooth walls. Full line = f_μ, dashed line = (1 - f_1)/20, dotted line = f_2. ▲ = DNS data for f_μ (Hwang & Lin, 1998), □ (PRS) = f_μ calculated using averaged data profiles from (Patel *et al*, 1985), + (PRS2) = f_μ recalculated values using a more realistic k-profile.

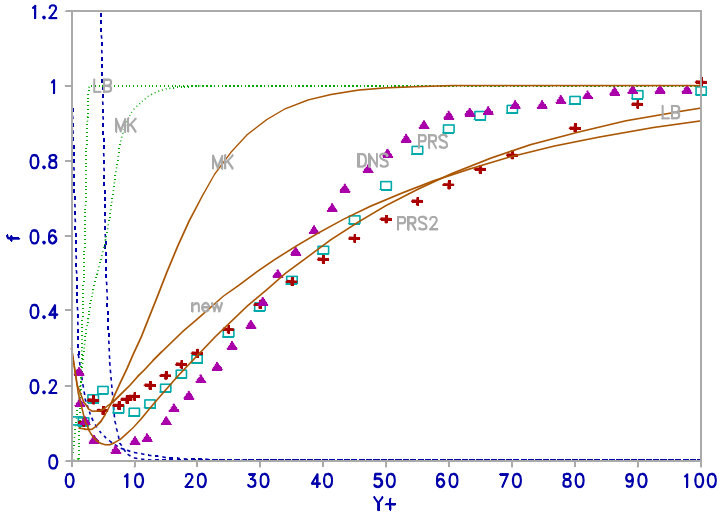

Figure 18. Fully developed turbulent flow of a clear fluid between smooth parallel plates. Comparison of various k-ε turbulence models (Toorman, 1998b).

REFERENCES

Abe, K., Y. Nagano & T. Kondo (1992). Numerical prediction of separating and re-attaching flows with a modified low-Reynolds-number k-ε model. *J. Wind. Eng.*, 52:213-218.

Batchelor, C.K. & Townsend, A.A. (1948). Decay of isotropic turbulence in the final period. *Proc. Roy. Soc. London*, Series A. 194:538ff.

Booij, R. (1992). *Turbulentie in de Waterloopkunde* (Turbulence in Hydraulics). Course B82 Textbook, Dept. of Civil Engineering, T.U.Delft, 141 pp. (in Dutch).

Bradshaw, P., B.E. Launder & J.L. Lumley (1996). Collaborative testing of turbulence models. *J. Fluids Engrg.* 118:243-247.

CHAM (1994). *PHOENICS Manual*. CHAM, Manchester.

Chen, C.-J. & S.-Y. Jaw (1998). *Fundamentals of turbulence modeling*. Taylor & Francis, Washington D.C., 292 pp.

Chen, H.C. & V.C. Patel (1988). Near-wall turbulence models for complex flows including separation. *AIAA J.* 26(6):641-648.

Chien, K.Y. (1982). Prediction of channel and boundary-layer flows with a low-Reynolds turbulence model. *AIAA J.*, 20:33-38.

Christensen, B.A. (1972). Incipient motion on cohesionless channel banks. In: *Sedimentation* (Symp. to honor H.A. Einstein, edited by H.S. Shen), pp.(4)1-22, Colorado State University, Fort Collins.

Comte-Bellot, G. (1965). Ecoulement turbulent entre deux parrois parallèles. *Publ. Scientifiques et Techniques* 419, Ministère de l'Air.

Davydov, B.I. (1961). *Sov. Phys. Dokl.*, 6(1):10-12.

De Mulder, T. (1997). Stabilized finite element methods for turbulent incompressible single-phase and dispersed two-phase flows. PhD thesis. Dept. Mech. Eng., K.U.Leuven, 234 pp.

Durbin, P.A. (1991). Near-wall turbulence closure modeling without 'damping functions'. *Theor. Comp. Fluid Dyn.*, 3:1ff.

Galland, J.C. (1996). Transport de sédiments en suspension et turbulence. Report He-42/96/007/A, Laboratoire National d'Hydraulique, EDF, Chatou (in French).

Goldberg, U. & Apsley, D. (1997). A wall-distance-free low Re k-ε turbulence model. *Comp. Meth. Appl. Mech. Engrg.*, 145:227-238.

Gust, G. (1976). Observations on turbulent drag reduction in a dilute suspension of clay in sea-water. *J. Fluid Mechanics*, 75(1):29-47.

Hanjalic, K. & Launder, B.E. (1976). Contribution towards a Reynolds-stress closure for low-Reynolds number turbulence. *J. Fluid Mech.*, 74:593-610.

Hassid, S. & Poreh, M. (1975). A turbulent energy model for flows with drag reduction. *J. Fluids Engrg.*, (June 1975):234-241.

Hughes, T.G. (1978). An investigation of turbulent flow problems using finite element methods. PhD thesis, University College of Swansea.

Hwang, C.B. & Lin, C.A. (1998). Improved low-Reynolds-number k-ε model based on direct numerical simulation data. *AIAA J.*, 36(1):38-43.

Jakobsen, F. (1989). The k-ε model: a review. Presented as PhD qualification test, University of Copenhagen.

Jaw, S.Y. (1991). Development of an anisotropic turbulence model for the prediction of complex flow. PhD thesis, Univ. of Iowa.

Kim, H.T., Kline, S.J. & Reynolds, W.C. (1968). An experimental study of turbulence production near a smooth wall in a turbulent boundary layer with zero pressure gradient. *Report* MD-20, Stanford University, CA.

Kim, J., Moin, P. & Moser, R.D. (1987). Turbulence statistics in fully developed channel

flow at low Reynolds number. *J. Fluid Mechanics*, 177:133-166.

Kim, J. (1989). Unpublished data, available through the CTTM data bank. (URL http://scholar.lib.vt.edu/ejournals/JFE/data/JFE/DB96-243/d4/simul1.dat)

Knowlton, B. (1999). Personal communication.

Kolmogorov, A.N. (1941). Local structure of turbulence in an incompressible fluid at very high Reynolds numbers. *Dokl. Akad. Nauk.* (Acad. of Sciences Report) 30(4):299-303 (in Russian).

Kolmogorov, A.N. (1942). Equations of turbulent motion of an incompressible fluid. *Seria Fizicheska Vi.*, No.1-2:56-58, Izv. Akad. Nauk. USSR (translation: Mech. Eng. Dept. Report ON/6, Imperial College, London, 1968).

Krogstad, P. (1991). Modification of the van Driest damping function to include the effects of surface roughness. *AIAA J.*, 29(6):888-894.

Lam, C. & Bremhorst, A. (1981). Modified form of the k-ε model for predicting wall turbulence. *J. Fluids Engineering*, 103:456-460.

Laufer, J. (1954). The structure of turbulence in fully developed pipe flow. *Report* 1174, N.A.C.A.

Launder, B.E. (1984). Dissipation and spectral transfer rates in turbulence. *Turbulence models and their applications*, Vol.1 (Launder et al.), pp.58-76.

Launder, B.E. & Sharma, B.I. (1974). Application of the energy-dissipation model of turbulence to the calculation of flow near a spinning disc. *Lett. Heat Mass Transfer*, 1:131-138.

Mohammadi, B. & Pironneau, O. (1993). *Analysis of the K-Epsilon turbulence model*. Research in Applied Mathematics Series, Masson, Paris, 196 pp.

Murakami, S., Kato, S., Chikamoto, T., Laurence, D. & Blay, D. (1996). New low-Reynolds-number k-ε model including damping effect due to buoyancy in a stratified flow field. *Int. J. Heat Mass Transfer*, 39(16):3483-3496.

Nagano, N. & Shimada, M. (1993). Modeling the dissipation-rate equation for two-equation turbulence model. *Proc. 9th Symp. on Turbulent Shear Flows* (Japan), Paper 23.2.

Nagano, Y. & Hishida, M. (1987). Improved form of the k-ε model for wall turbulent shear flow. *Trans. ASME*, 109:156-160.

Nagano, Y. & Tagawa, M. (1990). An improved k-ε model for boundary layer flows. *J. Fluids Engrg.*, 112:33-39.

Nikuradse, J. (1932). Gesetzmassigkeiten der turbulenten Stromung in glatten Rohren. (Regularities of turbulent flow in smooth pipes). *Forschungsarbeiten Ing. Wesen*, Vol.356 (in German).

Norris, L.H. and Reynolds, W.C. (1975). Turbulent channel flow with a moving wavyboundary. *Report* No. FM-10, Mech. Eng. Dept, Stanford University.

Park, T.S. & Sung, H.J. (1995). A nonlinear low-Reynolds-number k-ε model for turbulent separated and reattaching flows - I. Flow field computations. *Int. J. Heat Mass Transfer*, 38:2657-2666.

Patel, V.C., Rodi, W. & Scheuerer, G. (1985). Turbulence models for near-wall and low-Reynolds number flows: a review. *AIAA J.*, 23(9):1308-1319.

Pattijn, S., E. Dick and J. Steelant (1997). A quadratic low Reynolds number eddy viscosity turbulence model. *Proc. 4th Nat. Congr. Theoretical and Applied Mechanics* (Leuven, May 1997), pp.349-352.

Prandtl, L. (1945). Uber eines neues Formulsytem für die ausgebildete Turbulentz. *Nachr. Akad. Wiss., Math.-Phys. Klasse*, p.6, Göttingen.

Rhee, G.H. & Sung, H.J. (1996). A nonlinear low-Reynolds-number k-ε model for turbulent separated and reattaching flows - II. Thermal field computations. *Int. J. Heat Mass Transfer*, 39(16):3465-3474.

Rocabado, O.I. (1994). Computation of turbulent flows with the k-ε closure model. MEng. Thesis, Civil Eng. Dept., K.U.Leuven.

Rocabado, O.I. (1999). Modelling highly concentrated turbulent flows with non-cohesive sediments. PhD Thesis, Civil Eng. Dept., K.U.Leuven.

Rodi, W. (1972). The prediction of free boundary layers by use of a two-equation model of turbulence. *PhD thesis*, University of London.

Rodi, W. (1980). *Turbulence models and their application in hydraulics*. IAHR State-of-the-art Paper.

Rodi, W. (1988). Recent developments in turbulence modeling. *Proc. 3rd. Int. Symp. on Refined Flow Modeling and Turbulence Measurements* (Iwasa et al., eds.).

Rodi, W. (1991). Experience with two-layer models combining the k-ε model with a one-equation model near the wall. *AIAA 29th Aerospace Sciences Meeting*. Paper AIAA-91-0216.

Schubauer, G.B. (1954). Turbulent processes as observed in boundary layer and pipe. *J. Appl. Physics*, 25:188-194.

Sellin, R.H.J., J.W. Hoyt & O. Scrivener (1982). The effect of drag-reducing additives on fluid flows and their industrial applications. Part 1: Basic aspects. *J. Hydraulic Research*, 20(1):29-68.

Shames, I.H. (1982). *Mechanics of fluids*. McGraw Hill, New York.

So, R.M.C., Aksoy, H., Yuan, S.P. & Sommer, T.P. (1996). Modelling Reynolds-number effects in wall-bounded turbulent flows. *Trans. ASME*, 118:260-267.

Spalart, P.R. (1988). Direct simulation of a turbulent boundary layer up to $Re_\theta = 1410$. *J. Fluid Mech.*, 187:61-98.

Toms, B.A. (1949). Some observations on the flow of linear polymeric solutions through straight tubes at large Reynolds numbers. *Proc. 1st. Int. Congr. Rheology*, Amsterdam.

Toorman, E.A. (1997). Eddy viscosity models for sediment-laden turbulent flow. *ERCOFTAC Seminar on New Developments and Validation in Turbulence Modelling* (Gent, Dec.1997), 24 pp.

Toorman, E.A. (1998a). A numerical study of the effect of suspended cohesive sediment particles on turbulent open-channel flow. Presented at the *5th Int. Conf. on Nearshore and Estuarine Cohesive Sediment Transport* (INTERCOH'98, Seoul, Korea, May 1998), Book of Abstracts pp.68-69.

Toorman, E.A. (1998b). A study of modelling (near-wall) turbulence damping. *COSINUS Annual General Meeting* (Grenoble, Sept.1998), Book of Abstracts, pp.13-16.

Van Driest, E.R. (1956). On turbulent flow near a wall. *J. Aeronautical Sci.*, 23:1007-1011.

Vandromme, D. (1993). Turbulence modeling for compressible flows and implementation in Navier-Stokes solvers. *Introduction to the modeling of turbulence*. Lecture Series 1993-02, von Karman Institute, Brussels.

Wolfshtein, M. (1967). The velocity and temperature distribution of one-dimensional flow with turbulence augmentation and pressure gradient. *Int. J. Heat and Mass Transfer*, 12:301-318.

Yang, Z. & Shih, T.H. (1993). New time scale based k-ε model for near-wall turbulence. *AIAA J.*, 31(7):1191-1198.

Zhang, H., Faghri, M. & White, F.M. (1996). A new low-Reynolds-number k-ε model for turbulent flow over smooth and rough surfaces. *J. Fluids Engrg.*, 118:255-259.

Appendix 1: CHRISTENSEN'S MODIFIED LOG-LAW

A modification of the log-law, attempting to bridge the viscous sublayer, was proposed by Christensen (1972). The shear stress in the wall region is given by:

$$\tau = \ell^2 \left(\frac{\mathrm{d}u}{\mathrm{d}y} \right)^2 \qquad \textbf{(149)}$$

with a mixing length distribution which fulfils the limiting viscous condition at the wall:

$$\ell = \frac{\nu}{u_*} + \beta k_s + \kappa y \qquad \textbf{(150)}$$

where k_s = effective roughness height. Integration of the shear stress with as boundary conditions $u = 0$ at $y = 0$ and the log-law $u/u_* = \kappa^{-1}\ln(y/k_s) + B$ for large y yields:

$$\frac{u}{u_*} = \frac{1}{\kappa} \ln \left(1 + \frac{y}{k_s} \mathrm{e}^{\kappa B} \right) \qquad \textbf{(151)}$$

Christensen used the value $B = 8.5$ for a fixed sand bottom from Nikuradse (1932). Even though this equation yields a zero velocity at the wall, it does not fit experimental data in the viscous sublayer, because the assumption of a constant von Karman coefficient is invalid here.

Appendix 2: A CONTINUOUS LAW OF THE WALL

The construction of an analytical continuous law of the wall of the form $u_+(y_+)$ requires that the following conditions must be fulfilled. In the fully developed turbulent region the log-law must be reached. At the wall the following conditions hold: $u_+(0) = 0$, $u_+'(0) = 1$ and $u_+''(0) = 0$ (where a prime represents a derivation with regard to y_+). Consider the velocity profile of the form:

$$u_+ = F(y_+)\,G(y_+) = \left(1 - e^{-y_+/B(y_+)}\right)\left(y_1 + A\ln(1 + y_+/y_2)\right) \tag{152}$$

with: $F(0) = 0$ and $G(0) = y_1$. This profile guarantees the first wall condition. The velocity gradient is given by:

$$\frac{\mathrm{d}u_+}{\mathrm{d}y_+} = F\frac{\mathrm{d}G}{\mathrm{d}y_+} + \frac{\mathrm{d}F}{\mathrm{d}y_+}G \tag{153}$$

with:

$$\frac{\mathrm{d}F}{\mathrm{d}y_+} = \frac{e^{-y_+/B}}{B}\left(1 - \frac{y_+}{B}\frac{\mathrm{d}B}{\mathrm{d}y_+}\right) \tag{154}$$

which reaches a value of $1/B(0)$ at the wall (assuming that $B(0) \neq 0$), and:

$$\frac{\mathrm{d}G}{\mathrm{d}y_+} = \frac{A}{y_+ + y_2} \tag{155}$$

which reaches a value at the wall of A/y_2. In order to fulfil the first wall condition one finds the condition: $B(0) = y_1$. The second order derivative reads:

$$\frac{\mathrm{d}^2u_+}{\mathrm{d}y_+^2} = F\frac{\mathrm{d}^2G}{\mathrm{d}y_+^2} + G\frac{\mathrm{d}^2F}{\mathrm{d}y_+^2} + 2\frac{\mathrm{d}F}{\mathrm{d}y_+}\frac{\mathrm{d}G}{\mathrm{d}y_+} \tag{156}$$

with:

$$\begin{aligned}\frac{\mathrm{d}^2F}{\mathrm{d}y_+^2} &= \frac{1}{B}\frac{\mathrm{d}F}{\mathrm{d}y_+}\left(\left(\frac{y_+}{B} - 1\right)\frac{\mathrm{d}B}{\mathrm{d}y_+} - 1\right)\\ &- \frac{e^{-y_+/B}}{B^2}\left(\frac{\mathrm{d}B}{\mathrm{d}y_+}\left(1 - \frac{y_+}{B}\frac{\mathrm{d}B}{\mathrm{d}y_+}\right) + y_+\frac{\mathrm{d}^2B}{\mathrm{d}y_+^2}\right)\end{aligned} \tag{157}$$

which reaches a value of $1/B(0)^2$ at the wall, and:

$$\frac{\mathrm{d}^2G}{\mathrm{d}y_+^2} = -\frac{A}{(y_+ + y_2)^2} \tag{158}$$

The third wall condition leads to the condition:

$$\left(\frac{\mathrm{d}B}{\mathrm{d}y_+}\right)_{y_+=0} = \frac{A}{y_0} - \frac{1}{2} \qquad \textbf{(159)}$$

i.e. the derivative of B at the wall has a known value.

The most simple solution is to define $B(y_+) = y_1$, which implies that $y_2 = 2A$. The values of A and y_1 are determined by the condition that at large y_+ the log-law must be obtained. This immediately gives $A = 1/\tau$, the inverse von Karman coefficient. Hence: $y_2 = 2/\kappa$. The parameter y_1 is then found to be directly related to the equivalent roughness height by:

$$y_1 = A\ln(y_2) - \frac{1}{\kappa}\ln(y_0) = \frac{1}{\kappa}\ln(2/\kappa y_0) \qquad \textbf{(160)}$$

The problem with defining B constant is the fact that the corresponding velocity profile results in an underprediction of the Reynolds stress in the range $10 < y_+ < 40$. Surprisingly, in this range the experimental data of the velocity profile seem to be better approached than by the profile corresponding the Van Driest hypothesis, even though the latter gives a stress distribution which is closer to experimental data. One could play with various simple functions for $B(y_+)$.

Another simple way to construct a continuous law-of-the-wall is to make a superposition of the viscous and log laws multiplied with damping functions, i.e.:

$$u_+ = y_+\exp\left(\left(-(y_+/y_1)^m\right) + \frac{1}{\kappa}\ln\left(1+y_+/y_0\right)\left(1-\exp\left(-(y_+/y_2)^n\right)\right)\right) \qquad \textbf{(161)}$$

The corresponding velocity gradient is given by:

$$\frac{\mathrm{d}u_+}{\mathrm{d}y_+} = \mathrm{e}^{-(y_+/y_1)^m}\left(1-m(y_+/y_1)^m\right) + \frac{1-\mathrm{e}^{-(y_+/y_2)^n}}{\kappa(y_++y_0)} + \frac{n\,\mathrm{e}^{-(y_+/y_2)^n}}{\kappa y_+}\left(y_+/y_2\right)^n\ln\left(1+y_+/y_0\right) \qquad \textbf{(162)}$$

Relatively good fits can be obtained with various combinations of parameter values. The following set is preferred: $m = 1$, $n = 1$, $y_0 = 0.11$, $y_1 = 1$, $y_2 = 10$. The velocity gradient then reduces to:

$$\frac{\mathrm{d}u_+}{\mathrm{d}y_+} = \mathrm{e}^{-y_+/y_1}\left(1-y_+/y_1\right) + \frac{1-\mathrm{e}^{-y_+/y_2}}{\kappa\,(y_++y_0)} + \frac{\mathrm{e}^{-y_+/y_2}}{\kappa\,y_2}\ln\left(1+y_+/y_0\right) \qquad \textbf{(163)}$$

However, the gradient profile shows some anomalies in the viscous sublayer. The third wall condition requires that $y_1 = \kappa y_0 y_2$.